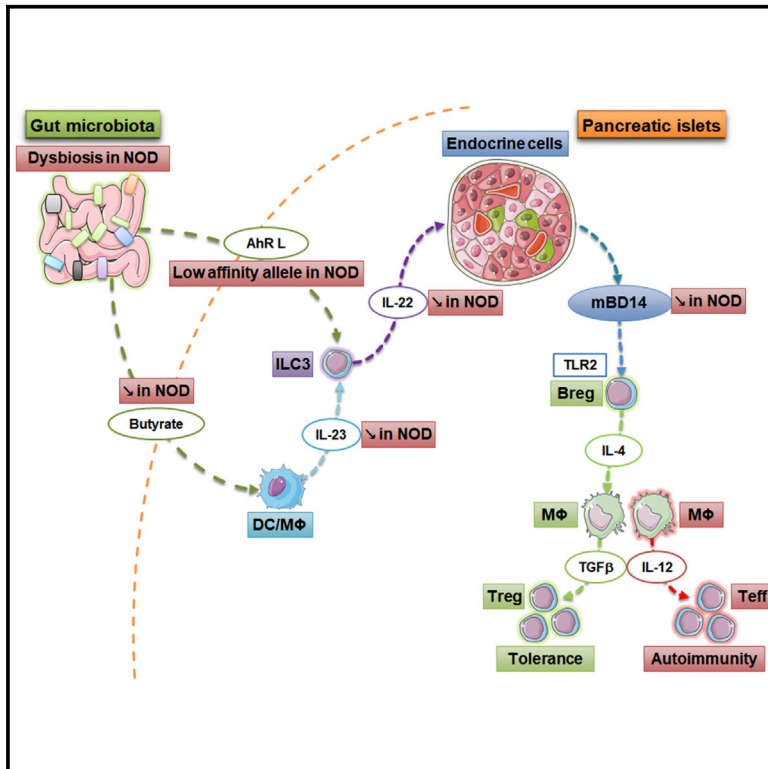


# Cell Metabolism

## Gut Microbiota-Stimulated Innate Lymphoid Cells Support $\beta$ -Defensin 14 Expression in Pancreatic Endocrine Cells, Preventing Autoimmune Diabetes

### Graphical Abstract



### Authors

Michela Miani, Julie Le Naour, Emmanuelle Waeckel-Enée, ..., Peter van Endert, Harry Sokol, Julien Diana

### Correspondence

julien.diana@inserm.fr

### In Brief

Miani et al. shed light on the complex interplay between the gut microbiota, immune cells, and the pancreas in autoimmune diabetes development. The gut microbiota promotes the expression of mouse  $\beta$ -defensin 14 (mBD14) by pancreatic endocrine cells, which play an immunoregulatory role preserving immune tolerance in the pancreas.

### Highlights

- MBD14 is expressed by pancreatic endocrine cells but poorly in NOD mice
- MBD14 treatment of NOD mice dampens the autoimmune response and diabetes
- Pancreatic innate lymphoid cells (ILCs) stimulate mBD14 expression via IL-22
- Gut microbiota-derived metabolites control IL-22 secretion by pancreatic ILCs



# Gut Microbiota-Stimulated Innate Lymphoid Cells Support $\beta$ -Defensin 14 Expression in Pancreatic Endocrine Cells, Preventing Autoimmune Diabetes

Michela Miani,<sup>1</sup> Julie Le Naour,<sup>1</sup> Emmanuelle Waeckel-Enée,<sup>1</sup> Subash chand Verma,<sup>1</sup> Marjolène Straube,<sup>2</sup> Patrick Emond,<sup>3,4</sup> Bernhard Ryffel,<sup>5,8</sup> Peter van Endert,<sup>1</sup> Harry Sokol,<sup>2,6,7</sup> and Julien Diana<sup>1,9,\*</sup>

<sup>1</sup>Institut Necker-Enfants Malades (INEM), Institut National de la Santé et de la Recherche Médicale (INSERM), Centre National de la Recherche Scientifique (CNRS), Sorbonne Universités, Paris, France

<sup>2</sup>Sorbonne Universités, École Normale Supérieure, CNRS, INSERM, Assistance Publique Hôpitaux de Paris (APHP) Laboratoire des Biomolécules (LBM), Paris, France

<sup>3</sup>UMR 1253, iBrain, Université de Tours, INSERM, Tours, France

<sup>4</sup>CHRU de Tours, Service de Médecine Nucléaire In Vitro, Tours, France

<sup>5</sup>Laboratory of Experimental and Molecular Immunology and Neurogenetics, UMR 7355 CNRS-University of Orleans, 3B, Orleans, France

<sup>6</sup>Micalis Institute, Institut National de la Recherche Agronomique (INRA), AgroParisTech, Université Paris-Saclay, Jouy-en-Josas, France

<sup>7</sup>Department of Gastroenterology, Saint Antoine Hospital, APHP, Paris, France

<sup>8</sup>IDM, Institute of Infectious Disease and Molecular Medicine, University of Cape Town, Cape Town, South Africa

<sup>9</sup>Lead Contact

\*Correspondence: [julien.diana@inserm.fr](mailto:julien.diana@inserm.fr)

<https://doi.org/10.1016/j.cmet.2018.06.012>

## SUMMARY

The gut microbiota is essential for the normal function of the gut immune system, and microbiota alterations are associated with autoimmune disorders. However, how the gut microbiota prevents autoimmunity in distant organs remains poorly defined. Here we reveal that gut microbiota conditioned innate lymphoid cells (ILCs) induce the expression of mouse  $\beta$ -defensin 14 (mBD14) by pancreatic endocrine cells, preventing autoimmune diabetes in the non-obese diabetic (NOD) mice. MBD14 stimulates, via Toll-like receptor 2, interleukin-4 (IL-4)-secreting B cells that induce regulatory macrophages, which in turn induce protective regulatory T cells. The gut microbiota-derived molecules, aryl hydrocarbon receptor (AHR) ligands and butyrate, promote IL-22 secretion by pancreatic ILCs, which induce expression of mBD14 by endocrine cells. Dysbiotic microbiota and low-affinity AHR allele explain the defective pancreatic expression of mBD14 observed in NOD mice. Our study reveals a yet unidentified crosstalk between ILCs and endocrine cells in the pancreas that is essential for the prevention of autoimmune diabetes development.

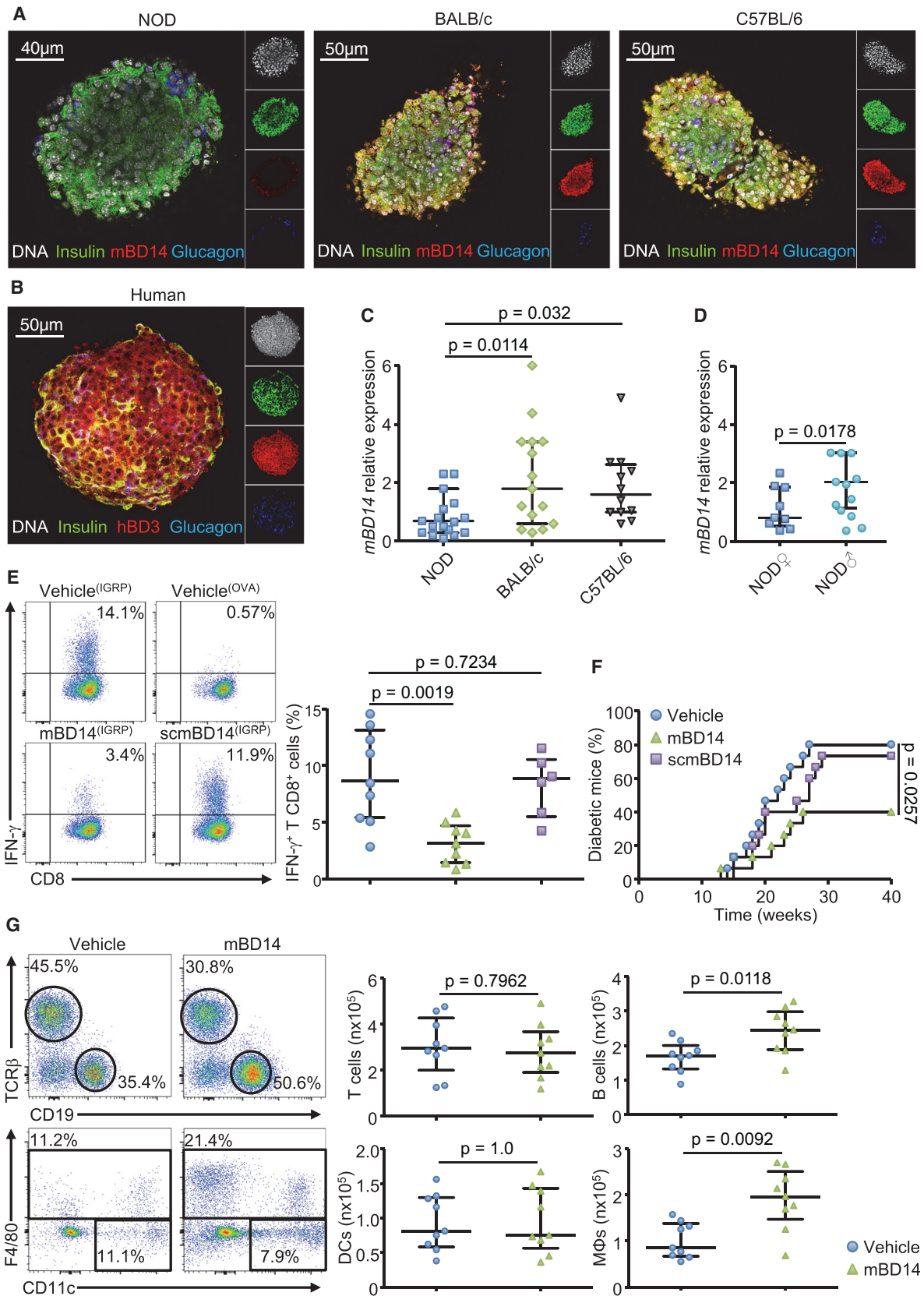
## INTRODUCTION

Antimicrobial peptides (AMPs), also called host defense peptides, are evolutionarily conserved molecules of the immune system found in almost all plants and animals. AMPs, mainly cathelicidins, defensins, and regenerating islet-derived pro-

teins, are mainly expressed at the epithelial surfaces, and due to their microbicide ability, AMPs play a critical role in fighting infection and in regulating the microbiota (Bevins and Salzman, 2011; Hancock et al., 2016; Ostaff et al., 2013; Zasloff, 2002; Zhang and Gallo, 2016). In the last decades, the ability of AMPs to modulate pro- and anti-inflammatory immune responses has been increasingly appreciated (Hancock et al., 2016; Zhang and Gallo, 2016). Not surprisingly, dysregulated expression of AMPs has been associated with autoinflammatory and autoimmune diseases such as atherosclerosis, systemic lupus erythematosus, rheumatoid arthritis, or type 1 diabetes (T1D) (Diana et al., 2013; Frasca and Lande, 2012; Kahlenberg and Kaplan, 2013). Recently, we have revealed the protective role of cathelicidin against autoimmune diabetes in the non-obese diabetic (NOD) mouse model. In diabetes-resistant mouse strains, cathelicidin is constitutively expressed by pancreatic endocrine cells and, owing to its immunoregulatory abilities, prevents pancreatic inflammation. We have further shown that pancreatic expression of cathelicidin is regulated by gut microbiota-derived metabolites and that, due to dysbiosis in NOD mice, pancreatic expression of cathelicidin is defective allowing the development of autoimmune diabetes (Sun et al., 2015).

While the recent literature highlights the role of cathelicidin in autoimmunity, how  $\beta$ -defensins may also modulate autoimmune diseases remains poorly investigated. A recent study demonstrates the protective role of mouse  $\beta$ -defensin 14 (mBD14) against experimental autoimmune encephalomyelitis (EAE) a mouse model of multiple sclerosis (Bruhs et al., 2016). We hypothesized that mBD14 may also play a role in the development of autoimmune diabetes in NOD mice. Here, we reveal that mBD14 is a part of a complex interplay between the gut microbiota, innate immune cells, and pancreatic endocrine cells, preserving immune tolerance in the pancreas and preventing autoimmune diabetes.





(legend on next page)

## RESULTS

### Pancreatic Endocrine Cells Express mBD14 in Non-autoimmune, but Not in NOD, Mice

$\beta$ -Defensins are known to be expressed by epithelial cells in the gut, skin, or lung, but their expression in the pancreas remains unknown (Ganz, 2003). Using confocal microscopy, we observed that mBD14 was expressed by pancreatic endocrine cells (glucagon<sup>+</sup>  $\alpha$  cells and insulin<sup>+</sup>  $\beta$  cells) with a lower expression in NOD mice compared with BALB/c and C57BL/6 mice (Figures 1A and S1A). Expression of human  $\beta$ -defensin 3 (hBD3), the ortholog of mBD14, was observed in pancreatic endocrine cells from healthy donors, in accordance with the evolutionary conserved nature of AMPs (Figure 1B). Interestingly, the expression of mBD14 mRNA in pancreatic islets was lower in NOD female mice compared with non-autoimmune female mice and lower in female NOD mice compared with male NOD mice (Figures 1C and 1D). These results suggest that mBD14 may play a protective role against autoimmune diabetes since male NOD mice are partially protected against the disease. These data prompted us to investigate whether mBD14 modulates the development of autoimmune diabetes in female NOD mice.

### mBD14 Is Protective against Autoimmune Diabetes in NOD Mice

We investigated whether administration of mBD14 modulates the development of autoimmune diabetes in NOD mice. RNA sequencing analysis revealed significant transcriptome changes in pancreatic islets of NOD mice after mBD14 administration. Noticeably, many genes related to inflammation were identified among downregulated genes in mBD14-treated NOD mice (Figures S2A and S2B). Flow cytometry analysis confirmed the anti-inflammatory effect of mBD14 in pancreatic islets, as administration of mBD14, but not of scrambled peptide (scmBD14), reduced the frequency of pancreatic interferon- $\gamma$  (IFN- $\gamma$ )<sup>+</sup> CD8<sup>+</sup> effector T cells specific for the  $\beta$  cell antigen islet-specific glucose-6-phosphatase catalytic subunit-related protein (IGRP)<sub>206-214</sub> (Figure 1E). Accordingly, treatment of prediabetic NOD mice with mBD14, but not with scmBD14, reduced the immune infiltration of the pancreatic islets and the incidence of autoimmune diabetes (Figures S1C and 1F). In addition, mBD14 treatment of hyperglycemic NOD mice resulted in a transient decrease of their glycemia (Figure S1B). To decipher how mBD14 regulated the diabetogenic immune response, we analyzed pancreatic immune cells from mBD14-treated NOD mice. mBD14 treatment significantly increased the number of B cells and macrophages,

while the number of dendritic cells (DCs) and T cells remained unchanged (Figures 1G and S1D). No significant difference was observed in the pancreatic lymph nodes (PLN) or in the spleen (Figures S1E and S1F). But the number of B cells in the PLN had a tendency to increase, suggesting that mBD14 may also impact B cells in this organ. Together, these data support a protective effect of mBD14 against autoimmune diabetes in NOD mice via the regulation of the diabetogenic response.

### mBD14 Induces Pancreatic Regulatory B Cells

To decipher the immunoregulatory effect of mBD14, we analyzed pancreatic B cells as their number significantly increased in mBD14-treated NOD mice. Although the precise role of B cells in T1D remains vague, it is believed that cytokine production and auto-antigen presentation by autoreactive B cells to self-reactive T cells play a significant role in the pathogenesis of T1D (Bloem and Roep, 2017). In addition, regulatory B (Breg) cell induction in pancreatic islets dampens the local inflammation and prevents disease development (Boldison and Wong, 2016). We observed that mBD14 treatment induced pancreatic B cell proliferation, as demonstrated by increased Ki67 expression (Figure 2A) and B cell recruitment, likely from PLN as shown by increased expression of CXCL13 mRNA (Figure S2C). Functionally, mBD14-induced B cells showed an increased expression of the regulatory molecules interleukin-4 (IL-4), active transforming growth factor  $\beta$  (TGF- $\beta$ ) LAP, and indoleamine 2,3-dioxygenase (IDO), while IL-10 expression was not significantly increased (Figure 2B). About 25% of B cells were double-positive for IDO and IL-4, with cells also expressing LAP. The induction of IL-4<sup>+</sup> B cells by mBD14 in pancreatic islets was dose dependent and not observed with scmBD14 (Figure S2D), and not observed in the PLN or the spleen (Figure S2E). Using an IL-4-neutralizing monoclonal antibody (mAb), we demonstrated that IL-4 was required for the protection against diabetes conferred by mBD14 treatment (Figure 2C). Breg cells are classically characterized by the expression of CD5 and other surface markers depending on the context studied (Mauri and Menon, 2015). IL-10<sup>+</sup> CD138<sup>+</sup> plasma cells were also described to be protective against EAE (Fillatreau et al., 2002). Here, IL-4<sup>+</sup> mBD14-induced B cells expressed CD5, CD1d, B220, CD21, and CD24, but were negative for CD138 (Figures 2D, 2E, S2F, and S2G). Next, using an *in vitro* system, we wanted to determine the receptor for mBD14 at the surface of pancreatic B cells. *In vitro*, mBD14 induced IL-4 and LAP expression in isolated B cells in a dose-dependent manner (Figure 2F). Using B cells from *myd88*<sup>-/-</sup> NOD mice, we found that mBD14 acted via TLRs and, more particularly, via the TLR1/2 heterodimer, as demonstrated by the use of

### Figure 1. mBD14 Is Expressed by Pancreatic Endocrine Cells and Is Protective against Autoimmune Diabetes

(A and B) Islets from female mice (A) or from female healthy subjects (B) were stained for insulin (green), mBD14 (A) or hBD3 (B) (red), glucagon (blue), and DNA (gray). Data are representative of six independent experiments.

(C and D) mRNA expression of mBD14 was analyzed by qRT-PCR in islets from female or male mice. Data are the median  $\pm$  interquartile range of 12–15 independent mice per group.

(E) IFN- $\gamma$  expression by OVA<sub>257-264</sub>-reactive (negative control) or IGRP<sub>206-214</sub>-reactive CD8<sup>+</sup> T cells were determined in islets from NOD mice treated with mBD14, scmBD14, or vehicle (d = 10). Data are the frequency of IFN- $\gamma$ <sup>+</sup> cells among the T cell population and are representative of the median  $\pm$  interquartile range of six to nine independent mice per group.

(F) Female NOD mice were treated with mBD14, scmBD14, or vehicle, and the incidence of diabetes was followed; n = 12 mice per group.

(G) Immune cell populations in islets from female NOD mice treated with mBD14 or vehicle (d = 3) were determined by flow cytometry. Data are the frequency of gated cells (CD19<sup>+</sup> B cell, TCR $\beta$ <sup>+</sup> T cell, F4/80<sup>-</sup> CD11c<sup>+</sup> DC, and F4/80<sup>+</sup> CD11b<sup>+</sup> macrophage) among the CD45<sup>+</sup> population (left panel) and the number of cells per mouse (right panel). Data are representative and are the median  $\pm$  interquartile range of nine independent mice per group.

See also Figures S1 and S2.

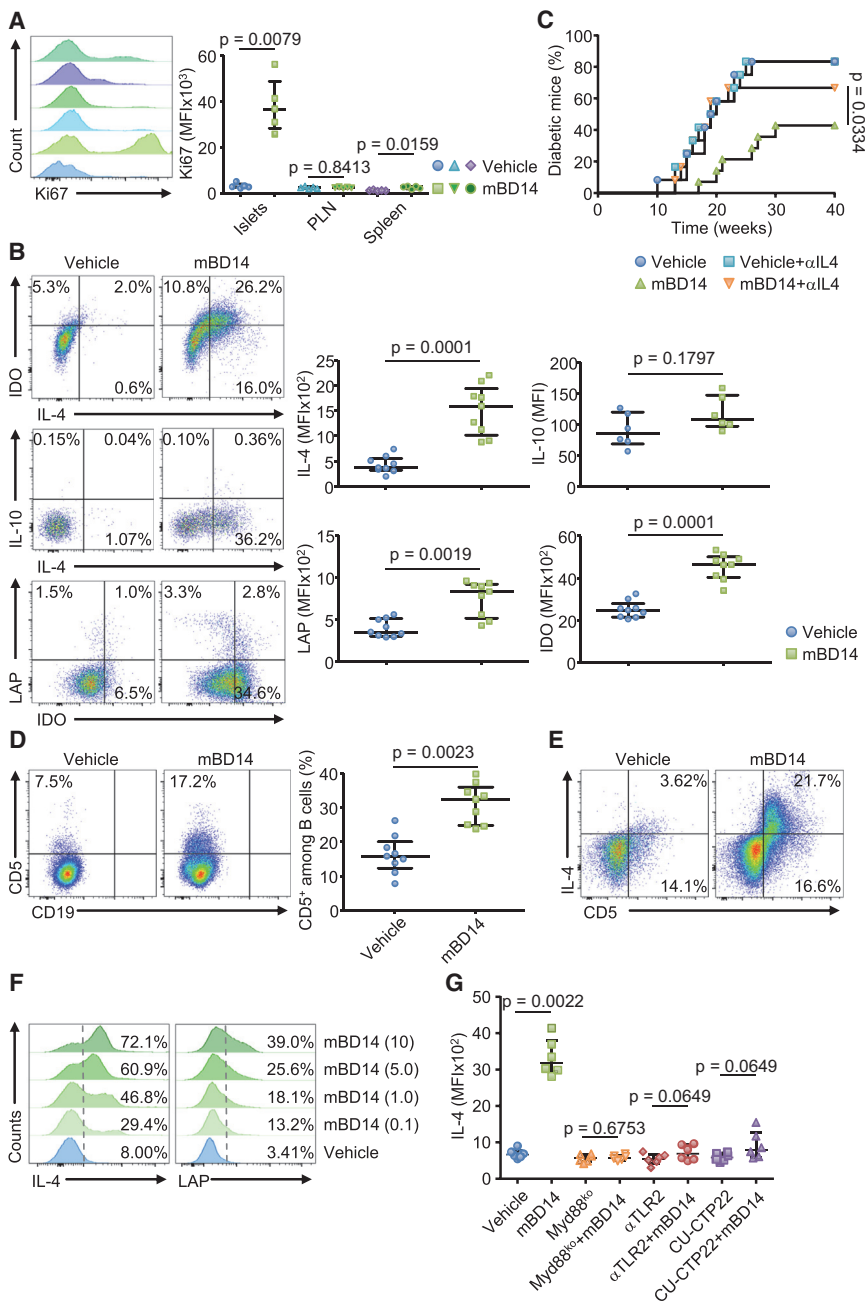


**Figure 2. MBD14 Induces Pancreatic Regulatory B Cells via TLR2**

(A, B, D, and E) NOD mice were treated with mBD14 or vehicle (d–3). B cells (CD19<sup>+</sup> CD11b<sup>–</sup>) from islets, lymph nodes, and spleen were analyzed by flow cytometry. Results show the frequency of positive cells and the mean fluorescence intensity (MFI) of the indicated marker among the B cell population. Data are representative and are the median  $\pm$  interquartile range of six to nine independent mice per group.

(C) Incidence of diabetes of NOD mice treated with mBD14 and anti-IL-4 neutralizing mAb.

(F and G) Pancreatic B cells from NOD mice were cultured for 4 days in the presence of growing dose ( $\mu$ g/mL) of mBD14 or vehicle. Results show the frequency of positive cells and the MFI of the indicated marker among B cells. Data are representative and are the median  $\pm$  interquartile range of five independent experiments with four mice pooled as source of B cells in each experiment. See also Figure S2.

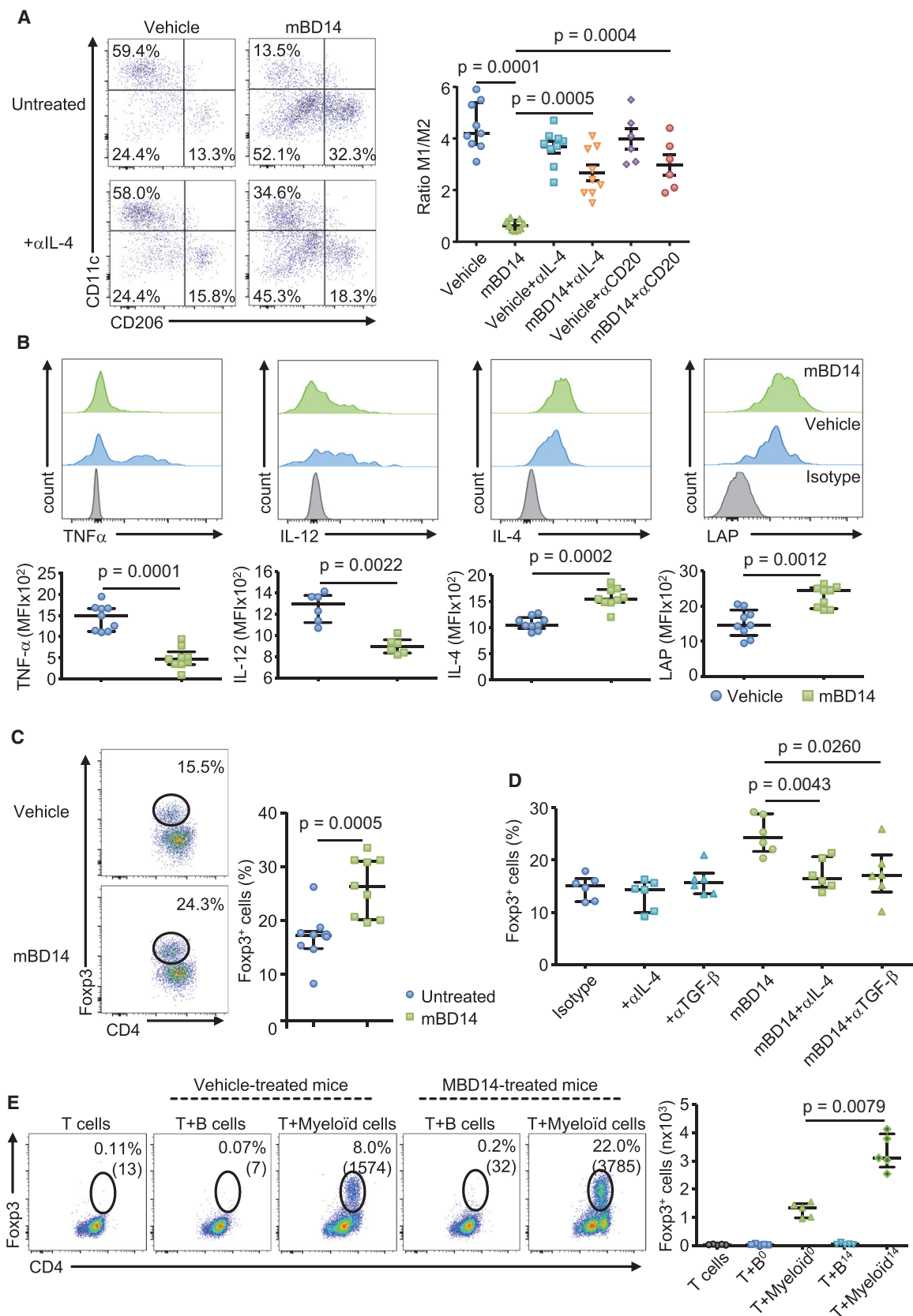
ter mBD14 treatment, we observed an increased frequency of pancreatic macrophages, likely due to the increased expression of the macrophage-recruiting chemokines CCL3 and CCL5 in pancreatic islets (Figure S3A). Interestingly, mBD14 treatment decreased the ratio between inflammatory CD11c<sup>+</sup> CD206<sup>–</sup> macrophages and regulatory CD206<sup>+</sup> CD11c<sup>–</sup> macrophages, and this decrease was dependent on IL-4 and B cells, as demonstrated by the use of an IL-4-neutralizing mAb and anti-CD20-depleting mAb (Figure 3A). Functionally, mBD14 treatment switched the expression of cytokines in pancreatic macrophages from an inflammatory profile (tumor necrosis factor alpha [TNF- $\alpha$ ] and IL-12) toward a regulatory profile (IL-4 and TGF- $\beta$ ) (Figure 3B) and induced the mRNA expression of arginase I and Ym1/Ym2, two markers of regulatory macrophages (Figure S3A). *In vitro*, we did not observe a direct effect of mBD14 on bone marrow-derived macro-

phages (Figure S3B), suggesting that the induction of regulatory macrophages by mBD14 was only dependent on IL-4-secreting B cells. DCs, the other main antigen-presenting cells in pancreatic islets, were also affected by mBD14 treatment with a reduction of IL-12 expression (Figure S3C). Both macrophages and DCs have the potential to induce regulatory T (Treg) cells necessary for a long-term protection against autoimmune diabetes (Tang and Bluestone, 2008). Ten days after mBD14 treatment, the frequency and number of Foxp3<sup>+</sup> Treg cells increased in pancreatic islets, but not in the PLN or the spleen (Figures 3C, S3D, and S3E). Using neutralizing antibodies, we demonstrated that induction of Treg cells by mBD14 was dependent on IL-4 and TGF- $\beta$ , two cytokines produced by mBD14-induced B cells and macrophages

### MBD14-Induced B Cells Promote Regulatory Macrophages and T Cells

Pancreatic mBD14-induced B cells were characterized by their high expression of IL-4, a cytokine known to drive macrophage polarization to a regulatory phenotype (Mantovani et al., 2007). Af-

phages (Figure S3B), suggesting that the induction of regulatory macrophages by mBD14 was only dependent on IL-4-secreting B cells. DCs, the other main antigen-presenting cells in pancreatic islets, were also affected by mBD14 treatment with a reduction of IL-12 expression (Figure S3C). Both macrophages and DCs have the potential to induce regulatory T (Treg) cells necessary for a long-term protection against autoimmune diabetes (Tang and Bluestone, 2008). Ten days after mBD14 treatment, the frequency and number of Foxp3<sup>+</sup> Treg cells increased in pancreatic islets, but not in the PLN or the spleen (Figures 3C, S3D, and S3E). Using neutralizing antibodies, we demonstrated that induction of Treg cells by mBD14 was dependent on IL-4 and TGF- $\beta$ , two cytokines produced by mBD14-induced B cells and macrophages



(legend on next page)

(Figure 3D). To determine the contribution of each cell type in Treg cell induction, we used an *in vitro* system. Isolated pancreatic myeloid cells (CD11b<sup>+</sup> cells) or B cells (CD19<sup>+</sup> cells) from vehicle- or mBD14-treated NOD mice were cultured with monoclonal naive (CD62L<sup>+</sup>) autoreactive BDC2.5 CD4<sup>+</sup> T cells devoid of Treg cells (CD25<sup>-</sup>). Myeloid cells, but not B cells, were able to induce Treg cells regardless their source. However, myeloid cells from mBD14-treated NOD mice had a significantly higher potency to induce Treg cells compared with their counterparts from vehicle-treated NOD mice (Figures 3E and S3F). We did not observe an induction of a regulatory phenotype in BDC2.5 T cells cultured alone with mBD14, excluding a direct effect of the peptide on these T cells (Figure S3G). Together, our data support that mBD14 induces an immunoregulatory cascade in pancreatic islets from B cells to Treg cells.

### IL-22 Promotes Pancreatic Expression of mBD14

We next sought to determine the pathway governing pancreatic expression of mBD14 and why this pathway was defective in NOD mice. In the gut, but also in other tissues including the pancreas, IL-22 has emerged as a key cytokine in tissue homeostasis partially through its ability to promote the production of AMPs (Aujla et al., 2008; Hill et al., 2013; Liang et al., 2006; Mulcahy et al., 2016; Sonnenberg et al., 2012; Wolk et al., 2004). The IL-22 receptor is highly expressed by pancreatic islets and  $\beta$  cells (Shioya et al., 2008; Wolk et al., 2004), and we hypothesized that IL-22 may induce mBD14 expression in pancreatic endocrine cells. We observed that IL-22 mRNA expression was reduced in pancreatic islets from female NOD mice compared with female non-autoimmune mice (Figure 4A) and male NOD mice (Figure S4A). The IL-22 level in the serum was also reduced in female NOD mice (Figure S4B). Importantly, the administration of IL-22Fc to NOD mice induced the expression of mBD14 mRNA in pancreatic islets (Figure 4B). *In vitro*, rIL-22 induced mBD14 by targeting directly mouse and human pancreatic islets (Figures 4C and 4D). Moreover, rIL-22 induced the expression of mBD14 in the Min6  $\beta$  cell line (Figure S4C). As described previously (Hill et al., 2013; Kinnebrew et al., 2012), IL-22Fc also stimulated the expression of the protective AMP Reg3 $\gamma$  in pancreatic islets and ileum (Figures S4D and S4E). Together, these data support that IL-22 induces the expression of mBD14 by pancreatic endocrine cells.

### Type 3 ILCs Are the Main Source of IL-22 in Pancreatic Islets

Both type 3 innate lymphoid cells (ILC3s) and conventional T cells can produce IL-22 (Sabat et al., 2014). By flow cytometry,

we investigated the ILC population in pancreatic islets from NOD, C57BL/6, and BALB/c mice. ILCs (CD127<sup>+</sup> CD90<sup>+</sup> Lin<sup>-</sup>) were observed in pancreatic islets of all mouse strains in equal number (Figure 4E). We confirmed these data using *rag*<sup>-/-</sup> mice to exclude a potential contamination with conventional T cells in our gating strategy (Figure S4F). Analyzing pancreatic ILC subtypes, we observed a reduction in the frequency of ROR $\gamma$ t<sup>+</sup> ILC3s in NOD mice compared with non-autoimmune mice (Figures 4F and S4G). Accordingly, the expression of IL-22 by pancreatic ILCs was reduced in NOD mice compared with non-autoimmune mice (Figures 4G and S4J). Conventional  $\alpha/\beta$  and  $\gamma/\delta$  T cells did not significantly express IL-22 in pancreatic islets from all mouse strains (Figures S4H–S4J). Using confocal microscopy, we observed the presence of IL-22<sup>+</sup> CD5<sup>-</sup> cells and IL-22<sup>-</sup> CD5<sup>+</sup> cells inside the pancreatic islets of C57BL/6 mice (Figures 4H and S5A). To confirm that only ILCs and not T cells were needed as an IL-22 source to induce mBD14 in the pancreatic islets, we treated C57BL/6 *rag*<sup>-/-</sup> mice with the IL-22 inducer IL-23. We observed that IL-23 efficiently increased mRNA expression of IL-22 and mBD14 in the pancreatic islets and ileum of these T cell-deficient mice (Figures S5B–S5E). The reduced frequency of ILC3s in NOD mice was not observed in pancreatic or mesenteric lymph nodes (MLNs) (Figures S6A and S6B). Furthermore, despite a high frequency of ILC3s in PLN or MLN of NOD mice, ILCs in these organs did not express higher levels of IL-22 compared with non-autoimmune strains, but rather expressed significantly higher levels of IFN- $\gamma$  and TNF- $\alpha$  (Figures S6C and S6D). Together, our data support that IL-22 production was defective in NOD mice, and that pancreatic ILC3s were the source of IL-22, promoting mBD14 expression in pancreatic islets of non-autoimmune mice.

### Gut Microbiota Controls IL-22 and mBD14 Expression in Pancreatic Islets

It is recognized that microbiota controls the production of IL-22 by ILC3s in the gut (Klose and Artis, 2016). To evaluate how gut microbiota may control IL-22 and consequently mBD14 expression in pancreatic islets, we treated BALB/c mice with a cocktail of broad-spectrum antibiotics (ABX) to reduce the gut microbiota. As described in the skin (Zanvit et al., 2015), ABX treatment decreased IL-22 protein levels in the serum and mRNA expression of IL-22 in pancreatic islets (Figures 5A and 5B). In parallel, ABX treatment decreased the expression of mBD14 mRNA in pancreatic islets, suggesting that the gut microbiota controlled the expression of mBD14 in pancreatic islets via the induction of IL-22 (Figure 5C). To confirm these data, we

### Figure 3. MBD14 Induces Pancreatic Regulatory Macrophages and Treg Cells

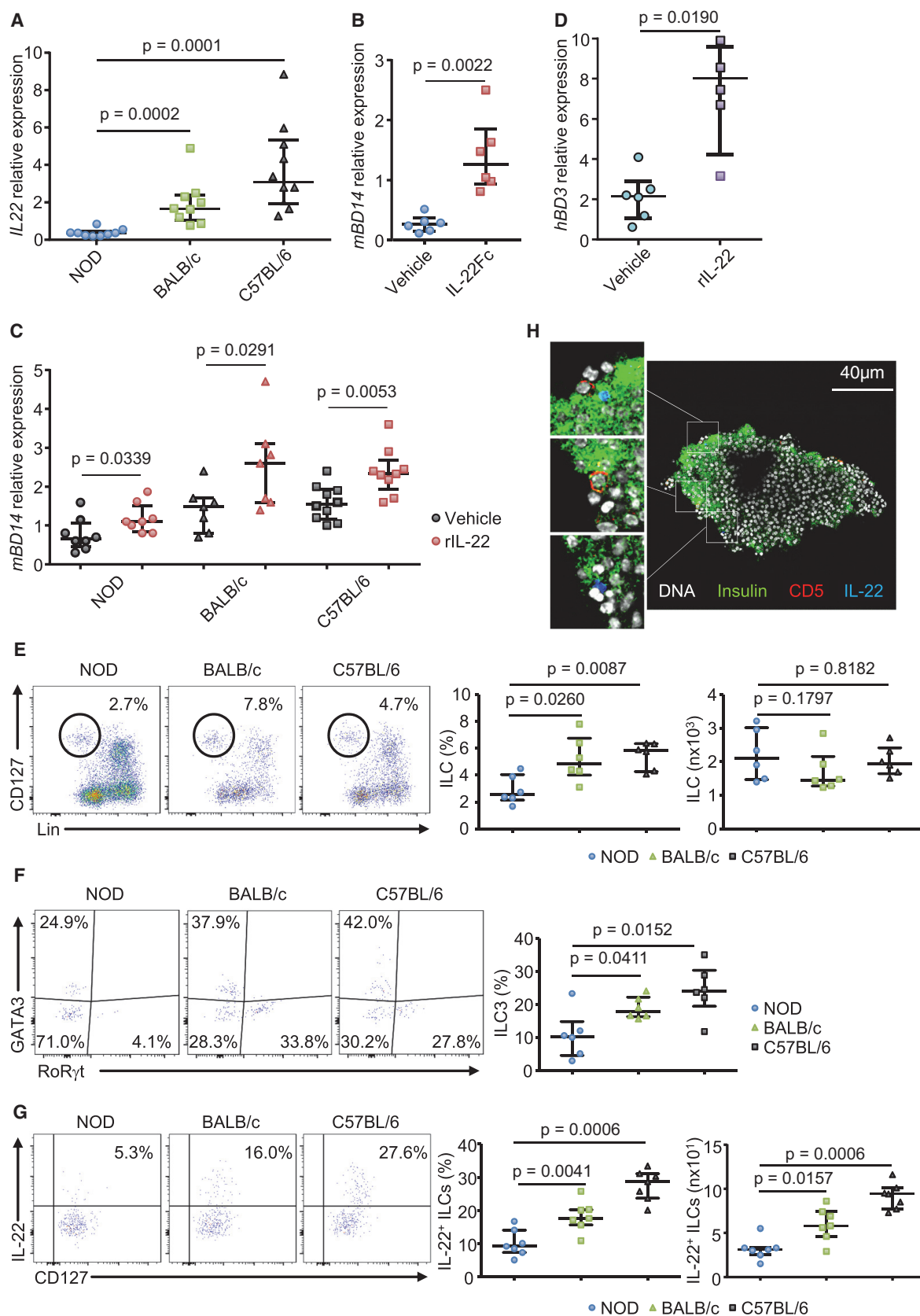
(A) Macrophage sub-populations in islets from NOD mice treated with mBD14 or vehicle (d–5) and treated with anti-IL-4 or anti-CD20 mAbs. Data show the frequency of gated cells among macrophages (F4/80<sup>+</sup> CD11b<sup>+</sup>) and the ratio between the frequency of inflammatory (M1, CD11c<sup>+</sup> CD206<sup>-</sup>) and regulatory (M2, CD11c<sup>-</sup> CD206<sup>+</sup>) macrophages. Data are representative and are the median  $\pm$  interquartile range of nine independent mice per group.

(B) Cytokine intracellular expression in pancreatic macrophages. Results show the MFI of indicated marker among macrophages. Data are representative and are the median  $\pm$  interquartile range of six to nine independent mice per group.

(C and D) Regulatory T cells were analyzed in islets from NOD mice treated with mBD14 or vehicle (day 10). In (D), mice were treated with anti-IL-4 or anti-TGF- $\beta$  neutralizing mAbs. Results show the frequency of Treg cells (Foxp3<sup>+</sup>) among the CD4<sup>+</sup> T cell population. Data are representative and are the median  $\pm$  interquartile range of six to nine independent mice per group.

(E) Pancreatic myeloid cells (CD11b<sup>+</sup>) or B cells (CD19<sup>+</sup>) were isolated from NOD mice treated with mBD14 (1<sup>4</sup>) or vehicle (0<sup>4</sup>) (d–4) and cultured with naive BDC2.5 T cells. Data show the frequency and number (in brackets) of Treg cells (Foxp3<sup>+</sup> CD25<sup>+</sup>) among the CD4 T cell population. Data are the median  $\pm$  interquartile range of five independent experiments with four mice pooled per group in each experiment.

See also Figure S3.



(legend on next page)

performed gut microbiota-transfer experiments. Expression of mBD14 and IL-22 mRNA was increased in pancreatic islets from NOD mice that received gut microbiota from BALB/c mice or C57BL/6 mice compared with NOD mice supplied with NOD gut microbiota (Figures 5D and S7A). Together, these data support that the gut microbiota controls the expression of mBD14 in pancreatic islets via IL-22 induction.

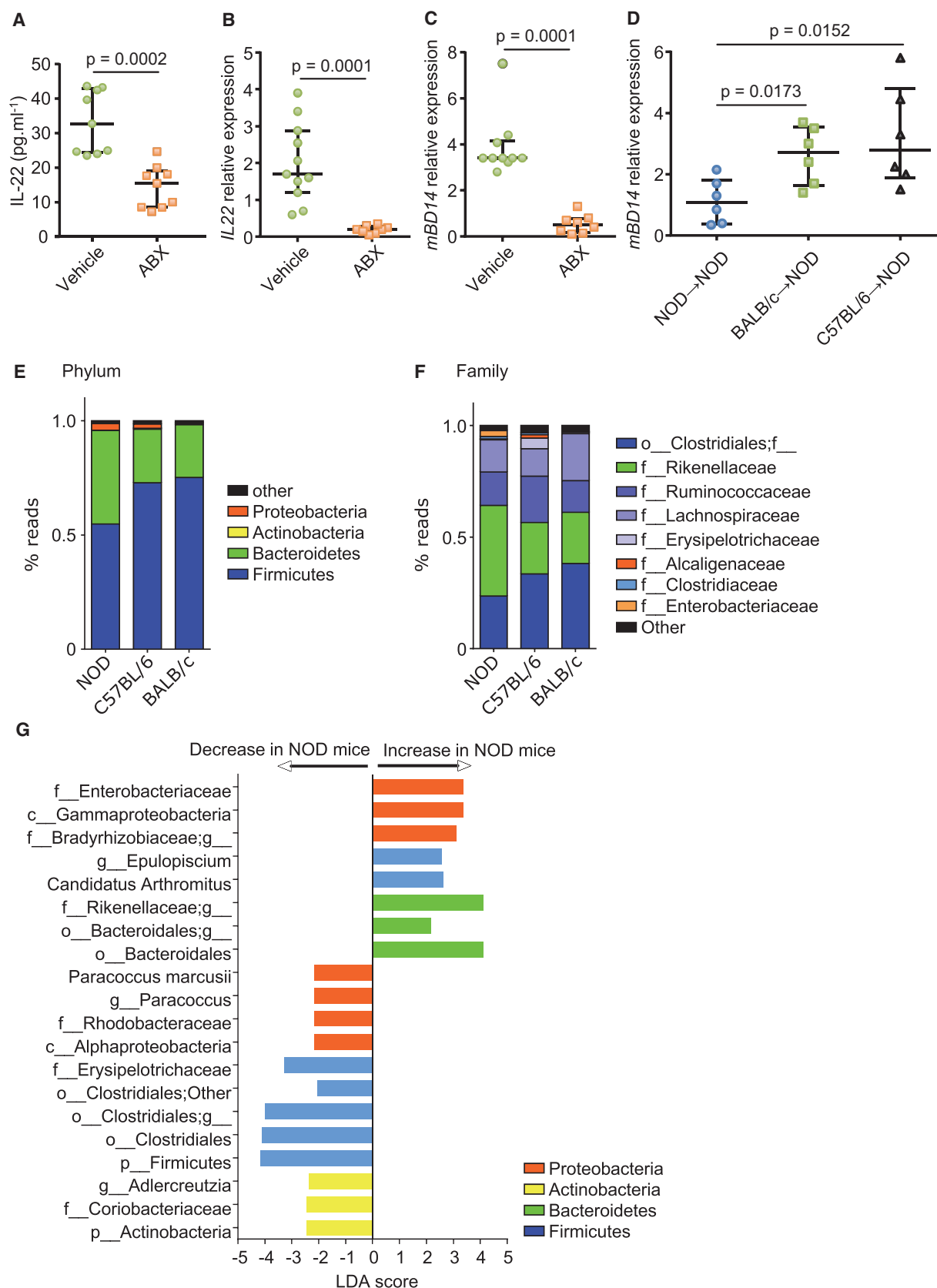
### Gut Microbiota Drives Pancreatic IL-22 Expression via AHR Ligands and IL-23

In the gut, microbiota controls the expression of IL-22 by ILC3s via different pathways (Zhou, 2016). Specific bacteria species produce aryl hydrocarbon receptor (AHR) ligands that directly activate ILC3s to produce IL-22. Other bacteria species produce metabolites that promote IL-23 secretion by intestinal phagocytes, and IL-23 activates ILC3s to produce IL-22. Consequently, we hypothesized that one or both of these pathways may be at play in pancreatic islets to stimulate the production of IL-22. To evaluate the ability of AHR ligand to stimulate mBD14 expression in pancreatic islets, we administered the AHR ligand 6-formylindolo-[3,2-b]-carbazole (FICZ) to BALB/c mice. FICZ administration induced mRNA expression of Cyp1a1 in pancreatic islets, confirming the activation of AHR<sup>+</sup> cells (Figure 6A), and increased the expression of IL-22 and mBD14 mRNA in pancreatic islets (Figures 6B and 6C). A similar induction of mBD14 was observed after injection of the AHR ligand indole-3-aldehyde, a tryptophan metabolite naturally produced by the gut microbiota (Figure 6C). As systemic AHR ligand administration may induce mBD14 in pancreatic islets via indirect pathways, we treated isolated pancreatic islets *in vitro* with FICZ and observed an increased expression of Cyp1a1, IL-22, and mBD14 mRNAs (Figures 6D–6F). The induction of pancreatic mBD14 by FICZ was dependent on IL-22, as demonstrated by the use of neutralizing mAb (Figure 6F) and by the fact that FICZ did not induce mBD14 expression in a Min6  $\beta$  cell line, excluding a direct role of AHR ligand on  $\beta$  cells (Figure 6G). Using a reporter assay, we failed to observe a significant defect in AHR ligand activity in the feces or the serum of NOD mice compared with non-autoimmune mice (Figures 6H and 6I). Similarly, using mass spectrometry, we did not detect significant difference in the concentration of various AHR ligands in the feces or the serum of NOD mice compared with non-autoimmune mice (Figure S7C). These data made it unlikely that a defective AHR ligand production in NOD mice may explain the defect in mBD14 expression in pancreatic islets. Nevertheless, the NOD strain expresses a low-affinity *AHR<sup>d</sup>* allele contrary to BALB/c or C57BL/6 strains carrying the *AHR<sup>p</sup>* allele (Kerkvliet et al., 2009; Okey et al.,

2005). Accordingly, by analyzing the expression of Cyp1a1 mRNA, we found that pancreatic islet cells from NOD mice were hyporesponsive to FICZ compared with BALB/c islet cells (Figure 6J). These data support that AHR ligands stimulated IL-22-secreting AHR<sup>+</sup> cells in pancreatic islets, inducing mBD14 expression, but in NOD mice, due to the presence of a low-affinity AHR allele, the level of AHR ligands may be insufficient to promote IL-22 and mBD14 expression. Then, we evaluated how IL-23 may also be implicated in the induction of mBD14 in pancreatic islets. Expression of IL-23 mRNA was reduced in pancreatic islets from NOD mice compared with BALB/c and C57BL/6 mice (Figure 7A), and IL-23 mRNA expression was increased in pancreatic islets from NOD mice that received gut microbiota from BALB/c mice or C57BL/6 mice compared with NOD mice supplied with NOD gut microbiota (Figure S7B). Flow cytometry analysis of pancreatic phagocytes confirmed a defective IL-23 expression in NOD mice compared with non-autoimmune strains (Figure 7B). In non-autoimmune mice, pancreatic IL-23 expression was mainly supported by macrophages (Figure S7D). Administration of rIL-23 to BALB/c mice increased the level of IL-22 in the serum was associated with an increased expression of IL-22 and mBD14 mRNA in pancreatic islets (Figures 7C–7E). Then we attempted to determine why pancreatic phagocytes failed to produce IL-23 in NOD mice. A recent study and our present data (Figure S7E) demonstrated the effect of butyrate, a microbiota-derived metabolite, in upregulating IL-23 expression in DCs and macrophages (Berndt et al., 2012). In addition, our previous study demonstrated that female NOD mice harbored reduced levels of butyrate in the serum and gut compared with non-autoimmune mice (Sun et al., 2015). Thus, we hypothesized that butyrate may stimulate the expression of IL-23 by pancreatic phagocytes, and that a defective production of butyrate in NOD mice may lead to reduced expression of pancreatic IL-23. By 16s rDNA sequencing from feces of NOD, BALB/c, and C57BL/6 mice, we observed that gut microbiota in NOD mice harbored a higher Bacteroidetes/Firmicutes ratio with a lower abundance of Clostridiales Lachnospiraceae, Ruminococcaceae, and Erysipelotrichaceae (Figures 5E–5G). These bacteria families are butyrogenic (Riviere et al., 2016), and their low abundance in NOD mice is in line with the low level of butyrate observed in this strain. Administration of butyrate to BALB/c mice increased the level of IL-23 in the serum and the expression of IL-23, IL-22, and mBD14 mRNA in pancreatic islets (Figures 7F–7I); however, we failed to observe a significant increase in the expression of mBD14 mRNA in butyrate-treated NOD mice (Figure S7F). *In vitro*, butyrate directly stimulated pancreatic islet cells to

### Figure 4. IL-22 Stimulates Pancreatic mBD14 Expression and Is Produced by Pancreatic ILCs

- (A) mRNA expression of IL-22 was analyzed by qRT-PCR in islets.  
 (B) mRNA expression of mBD14 in NOD mice treated with rmlL-22Fc or vehicle (h–3).  
 (C) mBD14 mRNA expression in isolated islets cultured in the presence of rmlL-22 (h–3).  
 (D) Human islets were cultured and analyzed as in (C).  
 (E) Innate lymphoid cells (ILCs) were analyzed in islets. Data show the frequency and number of ILCs (CD127<sup>+</sup> CD90<sup>+</sup> Lin<sup>-</sup>) among the CD45<sup>+</sup> population.  
 (F) The subtype of ILCs were analyzed in islets according to their expression of transcription factors. Data show the frequency of ILC3s (RoR $\gamma$ t<sup>+</sup> GATA3<sup>-</sup>) among the pancreatic ILC population. Data are representative and are the median  $\pm$  interquartile range of six independent mice per group.  
 (G) Data show the frequency and number of IL-22<sup>+</sup> cells among the pancreatic ILCs after stimulation with rmlL-23 plus PMA/ionomycin. Data are representative and are the median  $\pm$  interquartile range of seven independent mice per group.  
 (H) C57BL/6 islets were stained for insulin (green), CD5 (red), IL-22 (blue), and DNA (gray). Data are representative of five independent experiments. See also Figures S4–S6.



(legend on next page)

induce IL-23, IL-22, and mBD14 mRNA expression (Figures 7J–7L). This induction of mBD14 by butyrate was dependent on IL-22, as demonstrated by the use of neutralizing mAb (Figure 7L). *In vivo*, we observed that butyrate increased the expression of IL-23 by pancreatic phagocytes (Figure 7M). Since butyrate failed to induce mBD14 expression in the Min6  $\beta$  cell line (Figure S7G), we conclude that butyrate induced the expression of mBD14 in pancreatic islets via the stimulation of IL-23<sup>+</sup> phagocytes.

## DISCUSSION

The immunomodulatory role of AMPs is increasingly recognized, and their involvement in the immunopathology of autoimmune diseases is progressively identified (Kahlenberg and Kaplan, 2013; Mansour et al., 2014). Many studies have revealed the deleterious role of cathelicidin in autoinflammatory and autoimmune diseases, including atherosclerosis, small vessel vasculitis, psoriasis, and systemic lupus erythematosus (Gupta and Kaplan, 2016; Kahlenberg and Kaplan, 2013; Pinegin et al., 2015). In sterile condition, cathelicidin can be aberrantly expressed in the tissues by infiltrating neutrophils stimulating the uncontrolled production of type I IFNs, which are important contributors to autoimmunity (Hall and Rosen, 2010). We have shown that this pathway is also at play during the initiation of autoimmune diabetes in NOD mice (Diana et al., 2013); however, we have further demonstrated that cathelicidin may be also protective against autoimmune diabetes (Sun et al., 2015). Indeed, in non-autoimmune-prone mice, but not in NOD mice, cathelicidin is produced by pancreatic endocrine cells, and this endocrine cathelicidin exerts an immunoregulatory effect on macrophages, thereby preserving immune tolerance in the pancreas. Conversely, a recent study shows that the cathelicidin-like peptide FhHDM-1 from the helminth *Fasciola hepatica* regulates inflammatory macrophages, thus dampening the development of diabetes in NOD mice and the severity of EAE, a mouse model of multiple sclerosis (Lund et al., 2016). Collectively, these observations indicate that cathelicidin aberrantly produced from neutrophils is deleterious, while cathelicidin constitutively produced by non-immune cells or exogenous cathelicidin is protective against autoimmune diabetes. These opposite effects of cathelicidin from different cellular sources may be due to distinct post-translational modifications, which affect its function (Wang, 2012).

Like cathelicidin,  $\beta$ -defensins exert diverse immunomodulatory activities including receptor-mediated chemotaxis or modulation of immune cells via TLR, regulating both innate and adaptive immunity (Lehrer, 2004; Semple and Dorin, 2012). Studies in the Dorin laboratory of hBD3 have demonstrated that this

defensin inhibits the production of pro-inflammatory cytokines by LPS-primed macrophages *in vitro* and reduces the level of pro-inflammatory cytokines in the serum of LPS-treated mice when administrated *in vivo* (Semple et al., 2010, 2011). Studies from the group of Schwarz have shown the ability of mBD14 to induce Treg cells *in vitro* and *in vivo*, reducing the severity of EAE (Bruhs et al., 2016; Navid et al., 2012). Our present study reveals the direct effect of mBD14 on B cells via the TLR1/2 heterodimer, which is highly expressed on pancreatic CD5<sup>+</sup> B cells. Consistent with our finding, hBD3 activates human monocytes via the TLR1/2 heterodimer (Funderburg et al., 2007). Consequently, we cannot totally rule out a direct effect of mBD14 on pancreatic TLR2-expressing phagocytes. Together, the literature and our data support that  $\beta$ -defensins exert immunomodulatory function on different immune cell types, ensuring an efficient protection against tissue inflammation and autoimmunity.

Our data support that the protective role of mBD14 against autoimmune diabetes is mediated by induction of IL-4-producing B cells. In line with our results, transgenic expression of IL-4 by pancreatic  $\beta$  cells efficiently prevents the development of diabetes in NOD mice (Mueller et al., 1996). Using B cell-deficient NOD mice and depleting CD20 antibody, the pathogenic effect of B cells in autoimmune diabetes has been demonstrated (Xiu et al., 2008; Yang et al., 1997). However, various Breg subtypes play a protective role against several immune-related diseases including systemic lupus erythematosus, rheumatoid arthritis, and autoimmune diabetes (Rosser and Mauri, 2015). Reconciling these observations, the protective effect of B cell depletion against autoimmune diabetes is associated with the induction of IL-10-producing Breg cells in the reconstituted B cell population and the subsequent induction of Treg cells (Di Caro et al., 2014).

We show that IL-22 stimulates pancreatic  $\beta$  cells to express mBD14, and that IL-22 expression is defective in pancreatic islets of NOD mice. IL-22 is known to induce AMPs including  $\beta$ -defensins in different tissues (e.g., the gut, skin, and lung), preventing tissue damage (Aujla et al., 2008; Lindroos et al., 2011; Mulcahy et al., 2016; Wolk et al., 2006; Zheng et al., 2008). Pancreatic  $\beta$  cells highly express IL-22R (Shioya et al., 2008), and IL-22 is protective against metabolic disorders by improving  $\beta$  cell proliferation and function and by decreasing inflammation (Hasnain et al., 2014; Wang et al., 2014). In addition, IL-22 stimulates the expression of the AMPs Reg2 and Reg3 by pancreatic acinar cells, preventing tissue damage in a mouse model of pancreatitis (Aggarwal et al., 2001; Xue et al., 2012). In NOD mice, IL-22 promotes the expression of Reg1 and Reg2 by  $\beta$  cells, preventing  $\beta$  cell loss in an autocrine manner (Hill et al., 2013). Together, IL-22 induces different AMPs in pancreatic islets, promoting  $\beta$  cell function, regulating inflammation, and

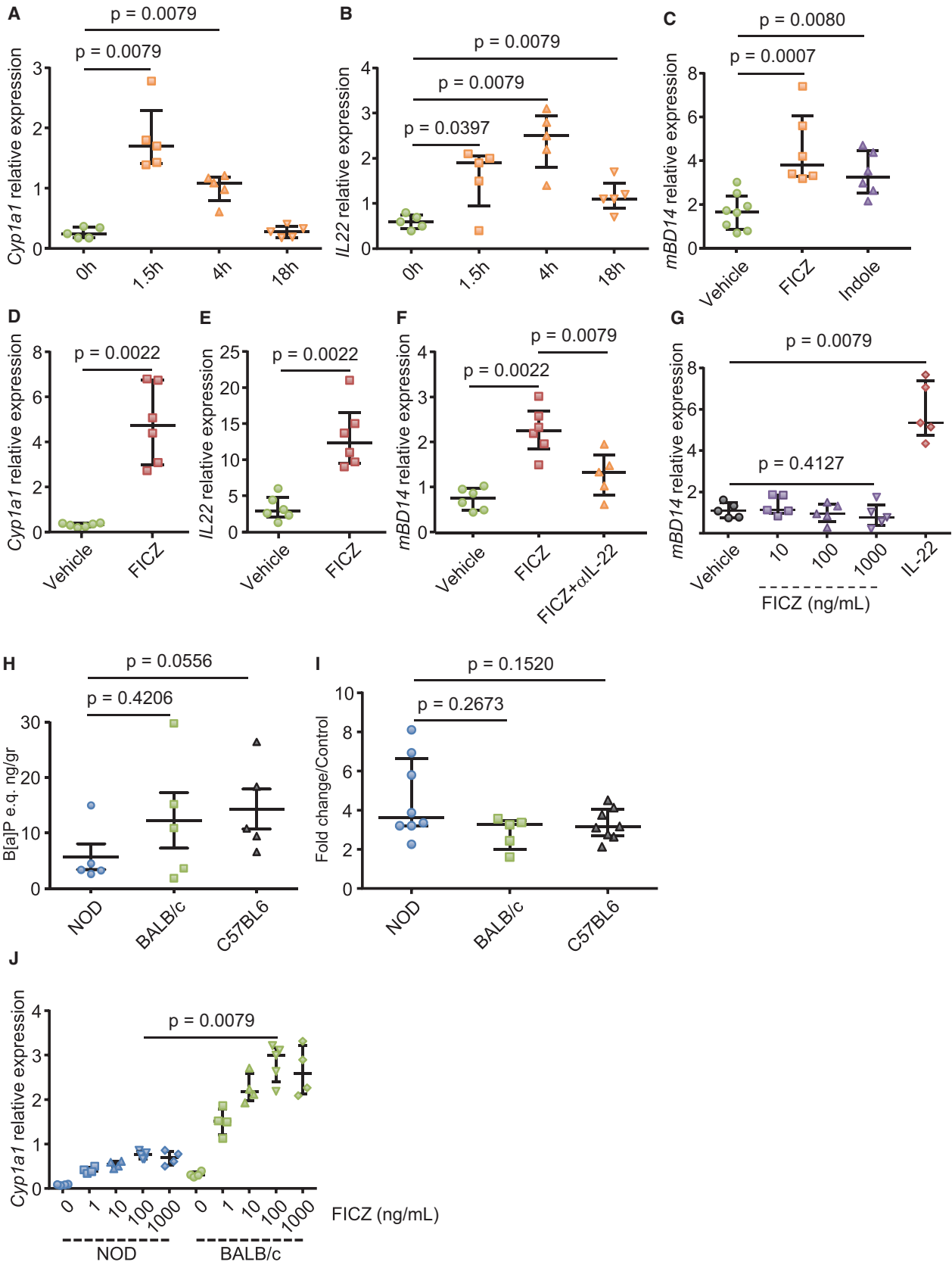
### Figure 5. Gut Microbiota Controls Pancreatic mBD14 Expression

(A–C) Six-week-old BALB/c mice were treated for 10 days with antibiotic cocktail (ABX). Seven days later, IL-22 concentration in the serum was determined by ELISA (A), and mRNA expression of IL-22 and mBD14 in the islets was determined by qRT-PCR (B and C). Data are the median  $\pm$  interquartile range of nine independent mice per group.

(D) Six-week-old NOD mice were transferred with gut microbiota from the different mouse strains ( $\rightarrow$ ). Seven days later, mRNA expression of mBD14 in islets was determined by qRT-PCR. Data are the median  $\pm$  interquartile range of six independent mice per group.

(E–G) Gut microbiota is altered in NOD mice. Gut microbiota composition was determined by 16S rDNA sequencing in the feces. Differential analysis (LEFSE) between mouse strains at the phylum level (E) and family level (F) is shown. (G) Differences in abundance are shown for the bacterial taxa in NOD mice (generated using the LEfSe pipeline). LDA, linear differential analysis; LEfSe, LDA effect size.

See also Figure S7.



(legend on next page)

preventing autoimmune response. The therapeutic use of IL-22 may be of interest against autoimmune diabetes. However, *IL22<sup>-/-</sup>* NOD mice did not display an increased incidence of autoimmune diabetes (Ishigame et al., 2013), but as shown here, NOD mice are characterized by a constitutively low level of pancreatic IL-22 so that genetic complete abrogation may not have a significant impact on the development of the disease. A recent study shows that IL-22 treatment of prediabetic NOD mice does not reduce the incidence of diabetes (Borg et al., 2017). However, as mentioned by the authors, a more pronounced effect may be obtained by increasing the dose, the frequency of administration, and by the use of a more metabolically stable Fc-based fusion protein, as used against metabolic diseases (Wang et al., 2014) and in our present study. Finally, the endogenous production of the neutralizing IL-22-binding protein may limit the therapeutic use of IL-22 at a lower dose (Martin et al., 2014).

We reveal for the first time the presence of IL-22-secreting ILC3s within pancreatic islets and their defect in NOD mice. In a mouse model of pancreatitis, AHR-reactive conventional T cells are a source of IL-22 in the whole pancreas (Xue et al., 2012); however, in the pancreatic islets we observe that  $\alpha/\beta$  or  $\gamma/\delta$  T cells did not express significant levels of IL-22. The role of ILCs in autoimmune diseases is an emerging field of research and, to our knowledge, the role of ILCs in autoimmune diabetes remains unknown. A deleterious role of IFN- $\gamma$ -producing ILC1s has been proposed in inflammatory bowel diseases, while IL-17-producing ILC3s may participate to rheumatic diseases, psoriasis, or multiple sclerosis (Shikhagaie et al., 2017). As autoimmune diabetes is not an IL-17-mediated disease (Bedoya et al., 2013), and due to the protective nature of IL-22, pancreatic ILC3s may play a protective role against autoimmune diabetes. Interestingly, despite a high number of ILC3s, ILCs in PLN or MLN of NOD mice did not express high levels of IL-22, but rather expressed significant levels of IFN- $\gamma$  and TNF- $\alpha$ . These data support that the inflammatory environment in the PLN and MLN in NOD mice may influence the cytokine expression of ILCs toward an inflammatory profile regardless of the subtype of ILCs, as already described in the gut (Melo-Gonzalez and Hepworth, 2017).

Finally, we show that the expression of IL-22 in pancreatic islets is under the control of the gut microbiota-derived molecules, AHR ligands and butyrate. NOD mice, such as the DBA/2 strain, carry a low-affinity *AHR<sup>d</sup>* genotype contrary to BALB/c or C57BL/6 mice carrying the *AHR<sup>b</sup>* allele. Consequently, *AHR<sup>d</sup>* mice require at least a 10-fold higher dose of

AHR ligand than *AHR<sup>b</sup>* mice to induce the same effects (Kerkvliet et al., 2009; Okey et al., 2005). These studies and our data support that AHR<sup>+</sup> cells in NOD mice are hyporesponsive to endogenous AHR ligands. Nevertheless, treatment of NOD mice with high doses of AHR ligand reduces insulinitis and the incidence of diabetes via the induction of regulatory AHR<sup>+</sup> DCs and Treg cells (Kerkvliet et al., 2009). The anti-inflammatory effect of AHR ligands is also mediated by the induction of IL-22 in various tissues including the gut, lung, and pancreas (Qiu et al., 2012; Simonian et al., 2010; Xue et al., 2012). Together, our data and the literature support a protective role for AHR-dependent IL-22 expression in the pancreas via the induction of AMPs promoting  $\beta$  cell regeneration and controlling inflammation.

As described in the gut (Abraham and Cho, 2009), we show that IL-23 induces IL-22 expression by ILC3s in pancreatic islets. We observed that IL-23 expression is reduced in pancreatic islets of NOD mice, as described in the serum of T1D patients (Roohi et al., 2014). Under the influence of gut microbiota-derived factors, resident intestinal phagocytes secrete IL-23, inducing, via IL-22, the expression of AMPs by epithelial cells (Caballero and Pamer, 2015; Honda and Littman, 2016). Here, we demonstrate that butyrate, a short-chain fatty acid classically produced by *Clostridia* species in the gut microbiota, stimulates the expression of IL-23 by pancreatic phagocytes, as described previously (Berndt et al., 2012). We have previously demonstrated that NOD mice harbor a reduced level of circulating butyrate (Sun et al., 2015), and we presently show that the gut microbiota of NOD mice is defective in butyrogenic bacteria, confirming previous reports in NOD mice and consistent with findings in children with  $\beta$  cell autoimmunity (Brown et al., 2016; de Goffau et al., 2013; Endesfelder et al., 2016; Giongo et al., 2011). Together, these data support that butyrate stimulates the production of immunoregulatory AMPs by pancreatic endocrine cells, preventing autoimmune diabetes. A recent study also demonstrated the protective role of butyrate against autoimmune diabetes in NOD mice through the expansion of colonic and splenic Treg cells (Marino et al., 2017). Considering the role of butyrate in promoting gut integrity and immune tolerance (Rooks and Garrett, 2016), this gut microbiota-derived metabolite appears as an attractive therapeutic candidate against T1D. Our studies and the literature highlight the beneficial relationships between the pancreas and the gut and this increasing knowledge should lead to identification of new approaches for the treatment of T1D (Tilg and Adolph, 2017).

#### Figure 6. AHR Ligands Stimulate Pancreatic mBD14 Expression

(A and B) Expression of Cyp1a1 and IL-22 mRNA was analyzed in islets from BALB/c mice treated with FICZ or vehicle for the indicated time points.

(C) Expression of mBD14 mRNA was analyzed in islets from BALB/c mice treated with FICZ, indole, or vehicle for 12 hr. Data are the median  $\pm$  interquartile of five independent mice per group.

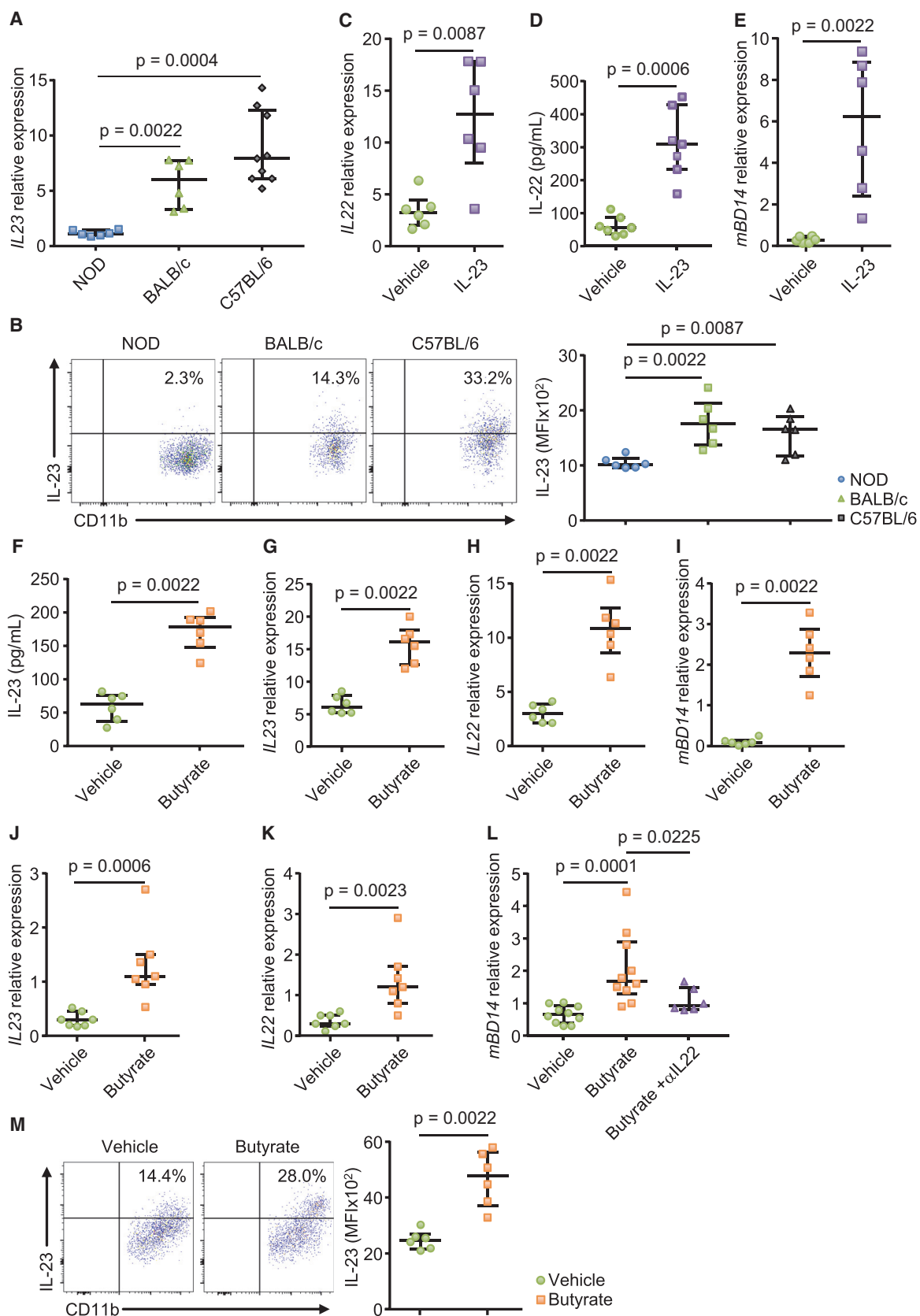
(D–F) Expression of Cyp1a1, IL-22, and mBD14 mRNA was determined in BALB/c islets cultured for 48 hr with FICZ and anti-IL-22 neutralizing mAb. Data are the median  $\pm$  interquartile of five to six independent mice per group.

(G) Min6  $\beta$  cells were treated with increasing doses of FICZ or IL-22 (200 ng/mL) for 24 hr. The expression of mBD14 mRNA was determined by qRT-PCR. Data are the median  $\pm$  interquartile of five independent experiments.

(H and I) AHR ligand activity was determined in the serum (H) and feces (I) using a reporter bioassay. Data are the median  $\pm$  interquartile of five to nine independent mice per group.

(J) mRNA expression of Cyp1a1 and mBD14 were determined in islets cultured for 48 hr with increasing doses (ng/mL) of FICZ. Data are the median  $\pm$  interquartile of four to five independent experiments with four mice pooled per group per experiment.

See also Figure S7.



(legend on next page)

### Limitation of the Study

Our study describes a complex interplay between innate immune cells, pancreatic endocrine cells, and the intestinal microbiota, participating in the prevention of autoimmune diabetes in NOD mice. Our data support that gut microbiota-stimulated ILCs, via the production of IL-22, promote the expression of immunoregulatory mBD14 by pancreatic endocrine cells. As the number of pancreatic ILCs is low, it would be important to confirm the presence of IL-22-producing ILCs in the pancreatic islets using reporter mice. The role of ILCs in autoimmune diseases is emerging, with both protective and deleterious roles described. To strengthen the protective role of pancreatic ILCs against autoimmune diabetes, transfer experiments would be helpful, although these experiments may be challenging due to the difficulty to obtain a sufficient number of ILCs from donor mice. Our group and others have described various pathways used by the gut microbiota to prevent autoimmune diabetes. Before transfer of these findings to the clinic, it would be important to determine the relative importance of each of these pathways in the prevention of the disease. Finally, as the well-characterized microbiome of laboratory mouse strain differs from human microbiome continuously facing environmental factors, it is critical to perform human studies to translate our findings to the human disease and envisage future therapies based on our conclusions.

### STAR★METHODS

Detailed methods are provided in the online version of this paper and include the following:

- KEY RESOURCES TABLE
- CONTACT FOR REAGENT AND RESOURCE SHARING
- EXPERIMENTAL MODEL AND SUBJECT DETAILS
  - Mice and Treatments
  - Spontaneous Diabetes Incidence
- METHOD DETAILS
  - Preparation of Pancreatic Islets
  - RT-qPCR
  - Flow Cytometry
  - Immunocytology
  - In Vitro B Cell Culture
  - In Vitro Treg Cell Induction
  - In Vitro Pancreatic Islet Culture
  - Cytokine Quantification
  - RNAseq Gene Expression Profiling

- AHR Ligand Activity Measurement
- Analysis of AHR Ligand Composition
- 16S rDNA Gene Sequencing
- QUANTIFICATION AND STATISTICAL ANALYSIS
  - 16S rDNA Gene Sequence Analysis
  - Statistical Analysis
- DATA AND SOFTWARE AVAILABILITY

### SUPPLEMENTAL INFORMATION

Supplemental Information includes seven figures and can be found with this article online at <https://doi.org/10.1016/j.cmet.2018.06.012>.

### ACKNOWLEDGMENTS

The authors greatly acknowledge Valérie Gaboriau-Routhiau (Institut Imagine, Paris, France), Marie Cherrier (INEM, Paris, France), Gaetan Barbet (Cornell University, New York, USA), and Nicolas Serafini (Institut Pasteur, Paris, France) for fruitful discussions. The authors acknowledge Antoine Lefevre (PST facility "Analyse des Systèmes Biologiques," Tours, France). The authors acknowledge the SFR Necker facilities (Paris, France), including Meriem Garfa-Traoré and Nicolas Goudin of the Imaging Facility, Christine Bole of the genomics facility, Nicolas Cagnard of the bioinformatics facility, and the team of the mouse facility (Hamburger Building). P.v.E. received funding from grants from Fondation pour la Recherche Médicale (DEQ20130326539), Idex Sorbonne Paris Cité, and Aide aux Jeunes Diabétiques. H.S. received funding from the European Research Council (ERC) under the European Union's Horizon 2020 research and innovation program (ERC-2016-StG-71577). J.D. received funding from the Juvenile Diabetes Research Foundation (JDRF)-SRA (2-SRA-2015-73-Q-R), the European Foundation for the Study of Diabetes (EFSD)/Lilly (94169), and the Association Française des Femmes Diabétiques (AFFD).

### AUTHOR CONTRIBUTIONS

M.M. designed, performed, and analyzed the experiments, with the general assistance of J.L.N., E.W.-E., and S.c.V. for confocal microscopy, histology, and cell culture. B.R. provided the *IL22<sup>-/-</sup>* C57BL/6 mice. P.E. performed the mass spectrometry experiments. M.S. and H.S. performed the gut microbiota analysis and AHR ligand analysis. P.v.E. and H.S. provided intellectual input. J.D. designed the project, performed experiments, interpreted data, and wrote the paper.

### DECLARATION OF INTERESTS

The authors declare no competing interests.

Received: January 5, 2018

Revised: April 19, 2018

Accepted: June 15, 2018

Published: July 12, 2018

### Figure 7. Butyrate Induces IL-23 Expression in the Pancreas, Stimulating mBD14 Expression

(A) IL-23 mRNA expression was determined in islets.

(B) Expression of IL-23 in pancreatic myeloid cells (CD11b<sup>+</sup> CD19<sup>-</sup>) was determined by flow cytometry. Results show the frequency of IL-23<sup>+</sup> cells and the MFI of IL-23 among myeloid cells. Data are representative and are the median ± interquartile range of six independent mice per group.

(C–E) mRNA expression of IL-22 and mBD14 was determined in islets from BALB/c mice treated with rmlL-23 (h=2) and the level of IL-22 was analyzed in the serum. Data are the median ± interquartile range of six to seven independent mice per group.

(F–I) Expression of IL-23, IL-22, and mBD14 mRNA was determined in islets from BALB/c mice treated with butyrate daily for 5 days. The level of IL-23 was determined in the serum. Data are the median ± interquartile of six independent mice per group.

(J–L) Expression of IL-23, IL-22, and mBD14 mRNA was determined in BALB/c islets cultured for 18 hr with butyrate and anti-IL-22 neutralizing mAb. Data are the median ± interquartile of five to seven independent mice per group.

(M) IL-23 expression by pancreatic myeloid cells was determined by flow cytometry in BALB/c mice treated with butyrate. Results show the frequency of IL-23<sup>+</sup> cells and the MFI of IL-23 among myeloid cells. Data are the median ± interquartile of six independent mice per group.

See also Figure S7.

## REFERENCES

- Abraham, C., and Cho, J.H. (2009). IL-23 and autoimmunity: new insights into the pathogenesis of inflammatory bowel disease. *Annu. Rev. Med.* 60, 97–110.
- Aggarwal, S., Xie, M.H., Maruoka, M., Foster, J., and Gurney, A.L. (2001). Acinar cells of the pancreas are a target of interleukin-22. *J. Interferon Cytokine Res.* 21, 1047–1053.
- Aujla, S.J., Chan, Y.R., Zheng, M., Fei, M., Askew, D.J., Pociask, D.A., Reinhart, T.A., McAllister, F., Edeal, J., Gaus, K., et al. (2008). IL-22 mediates mucosal host defense against Gram-negative bacterial pneumonia. *Nat. Med.* 14, 275–281.
- Bedoya, S.K., Lam, B., Lau, K., and Larkin, J., 3rd (2013). Th17 cells in immunity and autoimmunity. *Clin. Dev. Immunol.* 2013, 986789.
- Berndt, B.E., Zhang, M., Owyang, S.Y., Cole, T.S., Wang, T.W., Luther, J., Veniaminova, N.A., Merchant, J.L., Chen, C.C., Huffnagle, G.B., and Kao, J.Y. (2012). Butyrate increases IL-23 production by stimulated dendritic cells. *Am. J. Physiol. Gastrointest. Liver Physiol.* 303, G1384–G1392.
- Bevins, C.L., and Salzman, N.H. (2011). Paneth cells, antimicrobial peptides and maintenance of intestinal homeostasis. *Nat. Rev. Microbiol.* 9, 356–368.
- Bloem, S.J., and Roep, B.O. (2017). The elusive role of B lymphocytes and islet autoantibodies in (human) type 1 diabetes. *Diabetologia* 60, 1185–1189.
- Boldison, J., and Wong, F.S. (2016). Immune and pancreatic beta cell interactions in type 1 diabetes. *Trends Endocrinol. Metab.* 27, 856–867.
- Borg, D.J., Wang, R., Murray, L., Tong, H., Steptoe, R.J., McGuckin, M.A., and Hasnain, S.Z. (2017). The effect of interleukin-22 treatment on autoimmune diabetes in the NOD mouse. *Diabetologia* 60, 2256–2261.
- Brown, K., Godovanyi, A., Ma, C., Zhang, Y., Ahmadi-Vand, Z., Dai, C., Gorzelak, M.A., Chan, Y., Chan, J.M., Lochner, A., et al. (2016). Prolonged antibiotic treatment induces a diabetogenic intestinal microbiome that accelerates diabetes in NOD mice. *ISME J.* 10, 321–332.
- Bruhs, A., Schwarz, T., and Schwarz, A. (2016). Prevention and mitigation of experimental autoimmune encephalomyelitis by murine beta-defensins via induction of regulatory T cells. *J. Invest. Dermatol.* 136, 173–181.
- Caballero, S., and Pamer, E.G. (2015). Microbiota-mediated inflammation and antimicrobial defense in the intestine. *Annu. Rev. Immunol.* 33, 227–256.
- Caporaso, J.G., Kuczynski, J., Stombaugh, J., Bittinger, K., Bushman, F.D., Costello, E.K., Fierer, N., Pena, A.G., Goodrich, J.K., Gordon, J.I., et al. (2010). QIIME allows analysis of high-throughput community sequencing data. *Nat. Methods* 7, 335–336.
- de Goffau, M.C., Luopajarvi, K., Knip, M., Ilonen, J., Ruotula, T., Harkonen, T., Orivuori, L., Hakala, S., Welling, G.W., Harmsen, H.J., and Vaarala, O. (2013). Fecal microbiota composition differs between children with beta-cell autoimmunity and those without. *Diabetes* 62, 1238–1244.
- Di Caro, V., Phillips, B., Engman, C., Harnaha, J., Trucco, M., and Giannoukakis, N. (2014). Involvement of suppressive B-lymphocytes in the mechanism of tolerogenic dendritic cell reversal of type 1 diabetes in NOD mice. *PLoS One* 9, e83575.
- Diana, J., Simoni, Y., Furio, L., Beaudoin, L., Agerberth, B., Barrat, F., and Lehuen, A. (2013). Crosstalk between neutrophils, B-1a cells and plasmacytoid dendritic cells initiates autoimmune diabetes. *Nat. Med.* 19, 65–73.
- Edgar, R.C. (2010). Search and clustering orders of magnitude faster than BLAST. *Bioinformatics* 26, 2460–2461.
- Endesfelder, D., Engel, M., Davis-Richardson, A.G., Ardisson, A.N., Achenbach, P., Hummel, S., Winkler, C., Atkinson, M., Schatz, D., Triplett, E., et al. (2016). Towards a functional hypothesis relating anti-islet cell autoimmunity to the dietary impact on microbial communities and butyrate production. *Microbiome* 4, 17.
- Fillatreau, S., Sweeney, C.H., McGeachy, M.J., Gray, D., and Anderton, S.M. (2002). B cells regulate autoimmunity by provision of IL-10. *Nat. Immunol.* 3, 944–950.
- Frasca, L., and Lande, R. (2012). Role of defensins and cathelicidin LL37 in auto-immune and auto-inflammatory diseases. *Curr. Pharm. Biotechnol.* 13, 1882–1897.
- Funderburg, N., Lederman, M.M., Feng, Z., Drage, M.G., Jadlowsky, J., Harding, C.V., Weinberg, A., and Sieg, S.F. (2007). Human beta-defensin-3 activates professional antigen-presenting cells via Toll-like receptors 1 and 2. *Proc. Natl. Acad. Sci. USA* 104, 18631–18635.
- Ganz, T. (2003). Defensins: antimicrobial peptides of innate immunity. *Nat. Rev. Immunol.* 3, 710–720.
- Giongo, A., Gano, K.A., Crabb, D.B., Mukherjee, N., Novelo, L.L., Casella, G., Drew, J.C., Ilonen, J., Knip, M., Hyoty, H., et al. (2011). Toward defining the autoimmune microbiome for type 1 diabetes. *ISME J.* 5, 82–91.
- Gupta, S., and Kaplan, M.J. (2016). The role of neutrophils and NETosis in autoimmune and renal diseases. *Nat. Rev. Nephrol.* 12, 402–413.
- Hall, J.C., and Rosen, A. (2010). Type I interferons: crucial participants in disease amplification in autoimmunity. *Nat. Rev. Rheumatol.* 6, 40–49.
- Hancock, R.E., Haney, E.F., and Gill, E.E. (2016). The immunology of host defence peptides: beyond antimicrobial activity. *Nat. Rev. Immunol.* 16, 321–334.
- Hasnain, S.Z., Borg, D.J., Harcourt, B.E., Tong, H., Sheng, Y.H., Ng, C.P., Das, I., Wang, R., Chen, A.C., Loudovaris, T., et al. (2014). Glycemic control in diabetes is restored by therapeutic manipulation of cytokines that regulate beta cell stress. *Nat. Med.* 20, 1417–1426.
- Hill, T., Krougly, O., Nikoopour, E., Bellemore, S., Lee-Chan, E., Fouser, L.A., Hill, D.J., and Singh, B. (2013). The involvement of interleukin-22 in the expression of pancreatic beta cell regenerative Reg genes. *Cell. Regen. (Lond.)* 2, 2.
- Honda, K., and Littman, D.R. (2016). The microbiota in adaptive immune homeostasis and disease. *Nature* 535, 75–84.
- Ishigame, H., Zenewicz, L.A., Sanjabi, S., Licona-Limon, P., Nakayama, M., Leonard, W.J., and Flavell, R.A. (2013). Excessive Th1 responses due to the absence of TGF-beta signaling cause autoimmune diabetes and dysregulated Treg cell homeostasis. *Proc. Natl. Acad. Sci. USA* 110, 6961–6966.
- Kahlenberg, J.M., and Kaplan, M.J. (2013). Little peptide, big effects: the role of LL-37 in inflammation and autoimmune disease. *J. Immunol.* 191, 4895–4901.
- Kerkvliet, N.I., Stepan, L.B., Vorachek, W., Oda, S., Farrer, D., Wong, C.P., Pham, D., and Mourich, D.V. (2009). Activation of aryl hydrocarbon receptor by TCDD prevents diabetes in NOD mice and increases Foxp3+ T cells in pancreatic lymph nodes. *Immunotherapy* 1, 539–547.
- Kinnebrew, M.A., Buffie, C.G., Diehl, G.E., Zenewicz, L.A., Leiner, I., Hohl, T.M., Flavell, R.A., Littman, D.R., and Pamer, E.G. (2012). Interleukin 23 production by intestinal CD103(+)CD11b(+) dendritic cells in response to bacterial flagellin enhances mucosal innate immune defense. *Immunity* 36, 276–287.
- Klose, C.S., and Artis, D. (2016). Innate lymphoid cells as regulators of immunity, inflammation and tissue homeostasis. *Nat. Immunol.* 17, 765–774.
- Lamas, B., Richard, M.L., Leducq, V., Pham, H.P., Michel, M.L., Da Costa, G., Bridonneau, C., Jegou, S., Hoffmann, T.W., Natividad, J.M., et al. (2016). CARD9 impacts colitis by altering gut microbiota metabolism of tryptophan into aryl hydrocarbon receptor ligands. *Nat. Med.* 22, 598–605.
- Lehrer, R.I. (2004). Primate defensins. *Nat. Rev. Microbiol.* 2, 727–738.
- Liang, S.C., Tan, X.Y., Luxenberg, D.P., Karim, R., Dunussi-Joannopoulos, K., Collins, M., and Fouser, L.A. (2006). Interleukin (IL)-22 and IL-17 are coexpressed by Th17 cells and cooperatively enhance expression of antimicrobial peptides. *J. Exp. Med.* 203, 2271–2279.
- Lindroos, J., Svensson, L., Norsgaard, H., Lovato, P., Moller, K., Hagedorn, P.H., Olsen, G.M., and Labuda, T. (2011). IL-23-mediated epidermal hyperplasia is dependent on IL-6. *J. Invest. Dermatol.* 131, 1110–1118.
- Lund, M.E., Greer, J., Dixit, A., Alvarado, R., McCauley-Winter, P., To, J., Tanaka, A., Hutchinson, A.T., Robinson, M.W., Simpson, A.M., et al. (2016). A parasite-derived 68-mer peptide ameliorates autoimmune disease in murine models of type 1 diabetes and multiple sclerosis. *Sci. Rep.* 6, 37789.
- Mansour, S.C., Pena, O.M., and Hancock, R.E. (2014). Host defense peptides: front-line immunomodulators. *Trends Immunol.* 35, 443–450.
- Mantovani, A., Sica, A., and Locati, M. (2007). New vistas on macrophage differentiation and activation. *Eur. J. Immunol.* 37, 14–16.

- Marino, E., Richards, J.L., McLeod, K.H., Stanley, D., Yap, Y.A., Knight, J., McKenzie, C., Kranich, J., Oliveira, A.C., Rossello, F.J., et al. (2017). Gut microbial metabolites limit the frequency of autoimmune T cells and protect against type 1 diabetes. *Nat. Immunol.* **18**, 552–562.
- Martin, J.C., Beriou, G., Heslan, M., Chauvin, C., Utraiainen, L., Aumeunier, A., Scott, C.L., Mowat, A., Cerovic, V., Houston, S.A., et al. (2014). Interleukin-22 binding protein (IL-22BP) is constitutively expressed by a subset of conventional dendritic cells and is strongly induced by retinoic acid. *Mucosal Immunol.* **7**, 101–113.
- Mauri, C., and Menon, M. (2015). The expanding family of regulatory B cells. *Int. Immunol.* **27**, 479–486.
- McDonald, D., Price, M.N., Goodrich, J., Nawrocki, E.P., DeSantis, T.Z., Probst, A., Andersen, G.L., Knight, R., and Hugenholtz, P. (2012). An improved Greengenes taxonomy with explicit ranks for ecological and evolutionary analyses of bacteria and archaea. *ISME J.* **6**, 610–618.
- Melo-Gonzalez, F., and Hepworth, M.R. (2017). Functional and phenotypic heterogeneity of group 3 innate lymphoid cells. *Immunology* **150**, 265–275.
- Mueller, R., Krahl, T., and Sarvetnick, N. (1996). Pancreatic expression of interleukin-4 abrogates insulinitis and autoimmune diabetes in nonobese diabetic (NOD) mice. *J. Exp. Med.* **184**, 1093–1099.
- Mulcahy, M.E., Leech, J.M., Renaud, J.C., Mills, K.H., and McLoughlin, R.M. (2016). Interleukin-22 regulates antimicrobial peptide expression and keratinocyte differentiation to control *Staphylococcus aureus* colonization of the nasal mucosa. *Mucosal Immunol.* **9**, 1429–1441.
- Navid, F., Boniotto, M., Walker, C., Ahrens, K., Proksch, E., Sparwasser, T., Muller, W., Schwarz, T., and Schwarz, A. (2012). Induction of regulatory T cells by a murine beta-defensin. *J. Immunol.* **188**, 735–743.
- Okey, A.B., Franc, M.A., Moffat, I.D., Tijet, N., Boutros, P.C., Korkalainen, M., Tuomisto, J., and Pohjanvirta, R. (2005). Toxicological implications of polymorphisms in receptors for xenobiotic chemicals: the case of the aryl hydrocarbon receptor. *Toxicol. Appl. Pharmacol.* **207**, 43–51.
- Ostaf, M.J., Stange, E.F., and Wehkamp, J. (2013). Antimicrobial peptides and gut microbiota in homeostasis and pathology. *EMBO Mol. Med.* **5**, 1465–1483.
- Pieterse, B., Felzel, E., Winter, R., van der Burg, B., and Brouwer, A. (2013). PAH-CALUX, an optimized bioassay for AhR-mediated hazard identification of polycyclic aromatic hydrocarbons (PAHs) as individual compounds and in complex mixtures. *Environ. Sci. Technol.* **47**, 11651–11659.
- Pinegin, B., Vorobjeva, N., and Pinegin, V. (2015). Neutrophil extracellular traps and their role in the development of chronic inflammation and autoimmunity. *Autoimmun. Rev.* **14**, 633–640.
- Qiu, J., Heller, J.J., Guo, X., Chen, Z.M., Fish, K., Fu, Y.X., and Zhou, L. (2012). The aryl hydrocarbon receptor regulates gut immunity through modulation of innate lymphoid cells. *Immunity* **36**, 92–104.
- Riviere, A., Selak, M., Lantin, D., Leroy, F., and De Vuyst, L. (2016). Bifidobacteria and butyrate-producing colon bacteria: importance and strategies for their stimulation in the human gut. *Front. Microbiol.* **7**, 979.
- Roohi, A., Tabrizi, M., Abbasi, F., Ataie-Jafari, A., Nikbin, B., Larijani, B., Qorbani, M., Meysamie, A., Asgarian-Omran, H., Nikmanesh, B., et al. (2014). Serum IL-17, IL-23, and TGF-beta levels in type 1 and type 2 diabetic patients and age-matched healthy controls. *Biomed. Res. Int.* **2014**, 718946.
- Rooks, M.G., and Garrett, W.S. (2016). Gut microbiota, metabolites and host immunity. *Nat. Rev. Immunol.* **16**, 341–352.
- Rosser, E.C., and Mauri, C. (2015). Regulatory B cells: origin, phenotype, and function. *Immunity* **42**, 607–612.
- Sabat, R., Ouyang, W., and Wolk, K. (2014). Therapeutic opportunities of the IL-22-IL-22R1 system. *Nat. Rev. Drug Discov.* **13**, 21–38.
- Semple, F., and Dorin, J.R. (2012).  $\beta$ -Defensins: multifunctional modulators of infection, inflammation and more? *J. Innate Immun.* **4**, 337–348.
- Semple, F., MacPherson, H., Webb, S., Cox, S.L., Mallin, L.J., Tyrrell, C., Grimes, G.R., Semple, C.A., Nix, M.A., Millhauser, G.L., and Dorin, J.R. (2011). Human beta-defensin 3 affects the activity of pro-inflammatory pathways associated with MyD88 and TRIF. *Eur. J. Immunol.* **41**, 3291–3300.
- Semple, F., Webb, S., Li, H.N., Patel, H.B., Perretti, M., Jackson, I.J., Gray, M., Davidson, D.J., and Dorin, J.R. (2010). Human beta-defensin 3 has immunosuppressive activity in vitro and in vivo. *Eur. J. Immunol.* **40**, 1073–1078.
- Shikhagaie, M.M., Germar, K., Bal, S.M., Ros, X.R., and Spits, H. (2017). Innate lymphoid cells in autoimmunity: emerging regulators in rheumatic diseases. *Nat. Rev. Rheumatol.* **13**, 164–173.
- Shioya, M., Andoh, A., Kakinoki, S., Nishida, A., and Fujiyama, Y. (2008). Interleukin 22 receptor 1 expression in pancreas islets. *Pancreas* **36**, 197–199.
- Simonian, P.L., Wehrmann, F., Roark, C.L., Born, W.K., O'Brien, R.L., and Fontenot, A.P. (2010). Gammadelta T cells protect against lung fibrosis via IL-22. *J. Exp. Med.* **207**, 2239–2253.
- Sonnenberg, G.F., Monticelli, L.A., Alenghat, T., Fung, T.C., Hutnick, N.A., Kunisawa, J., Shibata, N., Grunberg, S., Sinha, R., Zahm, A.M., et al. (2012). Innate lymphoid cells promote anatomical containment of lymphoid-resident commensal bacteria. *Science* **336**, 1321–1325.
- Sun, J., Furio, L., Mecheri, R., van der Does, A.M., Lundberg, E., Saveanu, L., Chen, Y., van Ender, P., Agerberth, B., and Diana, J. (2015). Pancreatic beta-cells limit autoimmune diabetes via an immunoregulatory antimicrobial peptide expressed under the influence of the gut microbiota. *Immunity* **43**, 304–317.
- Tang, Q., and Bluestone, J.A. (2008). The Foxp3+ regulatory T cell: a jack of all trades, master of regulation. *Nat. Immunol.* **9**, 239–244.
- Tilg, H., and Adolph, T.E. (2017). Beyond digestion: the pancreas shapes intestinal microbiota and immunity. *Cell Metab.* **25**, 495–496.
- Wang, G. (2012). Post-translational modifications of natural antimicrobial peptides and strategies for peptide engineering. *Curr. Biotechnol.* **1**, 72–79.
- Wang, X., Ota, N., Manzanillo, P., Kates, L., Zavala-Solorio, J., Eidenschek, C., Zhang, J., Lesch, J., Lee, W.P., Ross, J., et al. (2014). Interleukin-22 alleviates metabolic disorders and restores mucosal immunity in diabetes. *Nature* **514**, 237–241.
- Wolk, K., Kunz, S., Witte, E., Friedrich, M., Asadullah, K., and Sabat, R. (2004). IL-22 increases the innate immunity of tissues. *Immunity* **21**, 241–254.
- Wolk, K., Witte, E., Wallace, E., Docke, W.D., Kunz, S., Asadullah, K., Volk, H.D., Sterry, W., and Sabat, R. (2006). IL-22 regulates the expression of genes responsible for antimicrobial defense, cellular differentiation, and mobility in keratinocytes: a potential role in psoriasis. *Eur. J. Immunol.* **36**, 1309–1323.
- Xiu, Y., Wong, C.P., Bouaziz, J.D., Hamaguchi, Y., Wang, Y., Pop, S.M., Tisch, R.M., and Tedder, T.F. (2008). B lymphocyte depletion by CD20 monoclonal antibody prevents diabetes in nonobese diabetic mice despite isotype-specific differences in Fc gamma R effector functions. *J. Immunol.* **180**, 2863–2875.
- Xue, J., Nguyen, D.T., and Habtezion, A. (2012). Aryl hydrocarbon receptor regulates pancreatic IL-22 production and protects mice from acute pancreatitis. *Gastroenterology* **143**, 1670–1680.
- Yang, M., Charlton, B., and Gautam, A.M. (1997). Development of insulinitis and diabetes in B cell-deficient NOD mice. *J. Autoimmun.* **10**, 257–260.
- Zanvit, P., Konkel, J.E., Jiao, X., Kasagi, S., Zhang, D., Wu, R., Chia, C., Ajami, N.J., Smith, D.P., Petrosino, J.F., et al. (2015). Antibiotics in neonatal life increase murine susceptibility to experimental psoriasis. *Nat. Commun.* **6**, 8424.
- Zaslloff, M. (2002). Antimicrobial peptides of multicellular organisms. *Nature* **415**, 389–395.
- Zhang, L.J., and Gallo, R.L. (2016). Antimicrobial peptides. *Curr. Biol.* **26**, R14–R19.
- Zhao, B., Bohonowych, J.E., Timme-Laragy, A., Jung, D., Affatato, A.A., Rice, R.H., Di Giulio, R.T., and Denison, M.S. (2013). Common commercial and consumer products contain activators of the aryl hydrocarbon (dioxin) receptor. *PLoS One* **8**, e56860.
- Zheng, Y., Valdez, P.A., Danilenko, D.M., Hu, Y., Sa, S.M., Gong, Q., Abbas, A.R., Modrusan, Z., Ghilardi, N., de Sauvage, F.J., and Ouyang, W. (2008). Interleukin-22 mediates early host defense against attaching and effacing bacterial pathogens. *Nat. Med.* **14**, 282–289.
- Zhou, L. (2016). AHR function in lymphocytes: emerging concepts. *Trends Immunol.* **37**, 17–31.

## STAR★METHODS

## KEY RESOURCES TABLE

REAGENT or RESOURCE	SOURCE	IDENTIFIER
Antibodies		
anti-CD16/CD32	Biolegend	Cat#101301; RRID: AB_312800
anti-CD45	Biolegend	Cat#103149; RRID: AB_2564590
anti-CD11b	Biolegend	Cat#101237; RRID: AB_11126744
anti-F4/80	Biolegend	Cat# 123113; RRID: AB_893490
anti-CD11c	Biolegend	Cat#117349; RRID: AB_2563905
anti-TCR $\beta$	Biolegend	Cat#109234; RRID: AB_2562350
anti-TCR $\gamma/\delta$	Biolegend	Cat#107512; RRID: AB_492900
anti-CD19	Biolegend	Cat#115549; RRID: AB_2563066
anti-CD206	Biolegend	Cat#141705; RRID: AB_10896421
anti-CD5	Miltenyi	Cat#130-102-574; RRID: AB_2658608
anti-CD1d	Biolegend	Cat#140805; RRID: AB_10643277
anti-CD21	Biolegend	Cat#123412; RRID: AB_2085160
anti-CD24	Biolegend	Cat#138503; RRID: AB_10576359
anti-CD138	Biolegend	Cat#142515; RRID: AB_2562336
anti-B220	Biolegend	Cat#103209; RRID: AB_312994
anti-TLR2	Biolegend	Cat#148603; RRID: AB_2564119
anti-CD127	Biolegend	Cat#135024; RRID: AB_11218800
anti-LAP	Biolegend	Cat#141409; RRID: AB_2561591
anti-TNF $\alpha$	Thermo Fisher Scientific	Cat#51-7321-82; RRID: AB_469813
anti-IL-12	Thermo Fisher Scientific	Cat#12-7123-41; RRID: AB_1963609
anti-IL-4	Thermo Fisher Scientific	Cat#12-7041-71; RRID: AB_466154
anti-IL-10	Thermo Fisher Scientific	Cat#51-7101-80; RRID: AB_469802
anti-IL-23	Thermo Fisher Scientific	Cat#50-7023-80; RRID: AB_10598203
anti-IDO	Biolegend	Cat#654003; RRID: AB_2564584
anti-IL-22	Biolegend	Cat#516404; RRID: AB_2124255
anti-CD4	BD	Cat#561025; RRID: AB_2034006
anti-CD8 $\alpha$	BD	Cat#553036; RRID: AB_394573
anti-IFN $\gamma$	Thermo Fisher Scientific	Cat#51-7311-82; RRID: AB_469809
anti-Foxp3	Thermo Fisher Scientific	Cat#51-5773-80; RRID: AB_469793
anti-RoR $\gamma$ t	Thermo Fisher Scientific	Cat#17-6981-80; RRID: AB_2573253
anti-GATA3	Biolegend	Cat#653812; RRID: AB_2563219
anti-Ki67	Thermo Fisher Scientific	Cat#50-5698-80; RRID: AB_2574234
anti-Insulin	Abcam	Cat#ab7842; RRID: AB_306130
anti-Glucagon	Abcam	Cat#ab10988; RRID: AB_297642
anti-CD5	Biolegend	Cat#100602; RRID: AB_312731
anti-mBD14	Mybiosource	Cat#MBS1490249; RRID: AB_2732866
anti-hBD3	Abcam	Cat#ab19270; RRID: AB_444821
anti-TLR2	Biolegend	Cat#309710; RRID: AB_2204581
anti-CD90.2	Thermo Fisher Scientific	Cat#17-5321-81; RRID: AB_469454
anti-Goat IgG	Biolegend	Cat#403006; RRID: AB_10567111
Goat anti-guinea pig	Thermo Fisher Scientific	Cat#A-11073; RRID: AB_142018
Goat anti-mouse	Thermo Fisher Scientific	Cat# A32728; RRID: AB_2633277
Goat anti-rabbit	Thermo Fisher Scientific	Cat#A32732; RRID: AB_2633281
Donkey anti-guinea pig	Jackson ImmunoResearch	Cat#706-545-148; RRID: AB_2340472

(Continued on next page)

**Continued**

REAGENT or RESOURCE	SOURCE	IDENTIFIER
Donkey anti-rat	Abcam	Cat#AB175475; RRID: AB_2636887
Donkey anti-goat	Thermo Fisher Scientific	Cat#A-21084; RRID: AB_2535741
anti-IL-4 mAb (Blocking/Neutralizing)	BioXcell	Cat#BE0045; RRID: AB_1107707
anti-TGF $\beta$ mAb (Blocking/Neutralizing)	BioXcell	Cat#BE0057; RRID: AB_1107757
anti-CD20 mAb (Blocking/Neutralizing)	BioXcell	Cat#BE0302; RRID: AB_2715460
anti-IL-22 mAb (Blocking/Neutralizing)	Thermo Fisher Scientific	Cat#16-7222-85; RRID: AB_2016574
anti-TLR2 mAb (Blocking/Neutralizing)	Invivogen	Cat#mab-hltr2; RRID: AB_763707
<b>Biological Samples</b>		
Human islets	Prodo laboratories	Cat#HIR-IEQ
<b>Chemicals, Peptides, and Recombinant Proteins</b>		
mBD14 peptide	Mybiosource	FLPKTLRKFRCRIRGGRCAVLNCL GKEEQIGRCSNSGRKCCRKKK
Scrambled mBD14 peptide	Proteogenix	LILRFCFLGTGCRGNLKVPRPARF CSRKEKKGKRSQINRCCKEGC
rmIL-22	Biologend	Cat#576208
rmIL-23	Biologend	Cat#589008
rmIL-22-Fc	Adipogen	Cat#CHI-MF-12022-C050
rmGM-CSF	R&D	Cat#415-ML-050
rmM-CSF	R&D	Cat#416-ML-050
6-Formylindolo-[3,2-b]-carbazole	Tocris	Cat#5304
Indole-3-carboxaldehyde	Sigma-Aldrich	Cat#129445
Sodium butyrate	Sigma-Aldrich	Cat#B5887
Lipopolysaccharides	Sigma-Aldrich	Cat#L6529
L-Cysteine hydrochloride	Sigma-Aldrich	Cat#30120
Collagenase P	Sigma-Aldrich	Cat#COLLP-RO ROCHE
Ficoll PM400	Sigma-Aldrich	Cat#F4375
Non-enzymatic cell dissociation solution	Sigma-Aldrich	Cat#C5789
DNase 1	Sigma-Aldrich	Cat#DN-25
<b>Critical Commercial Assays</b>		
Nucleospin RNA XS kit	Macherey-Nagel	Cat#740902.250
High capacity cDNA reverse transcription kit	Thermo Fisher	Cat#4368814
Takyon ROX SYBR MasterMix blue dTTP	Eurogentec	Cat#UF-RSMT-B0710
RNeasy Kit	QIAGEN	Cat#74106
IL-22 ELISA kit	Biologend	Cat#436304
IL-23 ELISA kit	Biologend	Cat#433707
Anti-biotin microbeads	Miltenyi	Cat#130-097-046
Naive CD4 <sup>+</sup> T cell isolation kit	Miltenyi	Cat#130-104-453
Foxp3 staining kit	Thermo Fisher Scientific	Cat#00-5523-00
True-Nuclear Transcription Factor kit	Biologend	Cat#424401
Glukotest kit	Roche	Accu-Chek Performa
<b>Deposited Data</b>		
RNA-seq data	Mendeley Data	<a href="https://doi.org/10.17632/4g2jdjxcff.1">https://doi.org/10.17632/4g2jdjxcff.1</a>
<b>Experimental Models: Cell Lines</b>		
Min 6 cells	ATCC	Cat#CRL-11506
<b>Experimental Models: Organisms/Strains</b>		
Mouse: NOD mice	Internal breeding	JAX: #001976
Mouse: NOD <i>rag</i> <sup>-/-</sup>	Internal breeding	MGI:97848
Mouse: NOD <i>myd88</i> <sup>-/-</sup>	Internal breeding	MGI:108005
Mouse: C57BL/6J	Internal breeding	JAX: #000664

(Continued on next page)

**Continued**

REAGENT or RESOURCE	SOURCE	IDENTIFIER
Mouse: C57BL/6J <i>rag</i> <sup>-/-</sup>	Internal breeding	JAX: #008309
Mouse: C57BL/6J <i>IL22</i> <sup>-/-</sup>	UMR7355, France	N/A
Mouse: BALB/cJ	Internal breeding	JAX: #000651
Oligonucleotides		
mGAPDH FW	Eurofins	5'-CCGTAGACAAAATGGTGAAGG-3'
mGAPDH REV	Eurofins	5'-CGTGAGTGGAGTCATACTGGA-3'
mBD14 FW	Eurofins	5'-GTATTCCTCATCTTGTCTTGG-3'
mBD14 REV	Eurofins	5'-AAGTACAGCACACCCGGCCAC-3'
IL22 FW	Eurofins	5'-CATGCAGGAGGTGGTACCTT-3'
IL22 REV	Eurofins	5'-CAGACGCAAGCATTCTCAG-3'
IL23 FW	Eurofins	5'-TGGTTGTGACCCACAAGGAC-3'
IL23 REV	Eurofins	5'-AGGGAGGTGTGAAGTTGCTC-3'
hBD3 FW	Eurofins	5'-CTTCTGTTTCTTTGCTCTTCC-3'
hBD3 REV	Eurofins	5'-CACTTGCCGATCTGTTCCTC-3'
Cyp1a1 FW	Eurofins	5'-CAGGATGTGTCTGGTTACTTTGAC-3'
Cyp1a1 REV	Eurofins	5'-CTGGGCTACACAAGACTCTGTCTC-3'
Reg3g FW	Eurofins	5'-TTCCTGTCTCCATGATCAAAA-3'
Reg3g REV	Eurofins	5'-CATCCACCTCTGTTGGGTTCA-3'
CCL3 FW	Eurofins	5'-CCTGCTGCTTCTCCTACAGC-3'
CCL3 REV	Eurofins	5'-CTGCCTCCAAGACTCTCAGG-3'
CCL5 FW	Eurofins	5'-CCCTCACCATCATCCTCACT-3'
CCL5 REV	Eurofins	5'-CCTTCGAGTGACAAACACGA-3'
CXCL9 FW	Eurofins	5'-CTGGGCAGAAGTCCGTCCTT-3'
CXCL9 REV	Eurofins	5'-TTACCGAAGGGAGGTGGACA-3'
CXCL10 FW	Eurofins	5'-GTCTGAGTCTCGCTCAAGT-3'
CXCL10 REV	Eurofins	5'-TCGCACCTCCACATAGCTTAC-3'
CXCL13 FW	Eurofins	5'-GAATGCTCAAGTCCGTTGC-3'
CXCL13 REV	Eurofins	5'-TGGGTTGTCACTAAATGCCTGT-3'
Software and Algorithms		
Prism v.6	Graphpad	<a href="https://www.graphpad.com/">https://www.graphpad.com/</a>
FlowJo v. 10	FlowJo, LLC	<a href="https://www.flowjo.com/">https://www.flowjo.com/</a>
Icy v.1.9.7.0	Institut Pasteur	<a href="http://icy.bioimageanalysis.org/">http://icy.bioimageanalysis.org/</a>

**CONTACT FOR REAGENT AND RESOURCE SHARING**

Further information and requests for resources and reagents should be directed to and will be fulfilled by the Lead Contact, Julien Diana ([julien.diana@inserm.fr](mailto:julien.diana@inserm.fr)).

**EXPERIMENTAL MODEL AND SUBJECT DETAILS****Mice and Treatments**

Female BALB/c, C57BL/6J, NOD, NOD *rag*<sup>-/-</sup>, C57BL/6J *rag*<sup>-/-</sup>, C57BL/6J *IL22*<sup>-/-</sup> and NOD *myd88*<sup>-/-</sup> mice between 10 and 12 weeks of age were used, bred and housed in specific pathogen-free conditions. In some experiments, male mice were used as indicated in the figure. Recombinant mBD14 (Mybiosource) (FLPKTLRKFCCRIRGGRCAVLNCLGKEEQIGRCSNSGRKCCRKKK), and scrambled (sc) mBD14 (Proteogenix) (LILRFLCFLGTGCRGNLKVPRARFCSRKEKKGKRSQINRCKEKG) were produced under aseptic conditions and provided after endotoxin removal processing. Peptides were administrated intraperitoneally (i.p.) at the dose of 10 µg diluted in 200 µl of vehicle (PBS-1% H<sub>2</sub>O). For *in vivo* blocking experiments, mice were treated (200 µg per i.p. injection at day -1, 1 and 3 post mBD14 treatment) with anti-IL4 (11B11) or anti-TGFβ (1D11) mAbs (BioXcell) or relevant isotype controls. For *in vivo* depleting experiments, mice were treated (200 µg per i.p. injection at day 0 and 1 post mBD14 treatment) with anti-CD20 (SA271G2) mAb (Biolegend) or relevant isotype controls. In some experiments, mice were i.p. injected with: rmlL-22Fc (Adipogen),

200  $\mu\text{g}$  in 200  $\mu\text{L}$  PBS for 3 h; rmlL-23 (Biolegend), 2  $\mu\text{g}$  in 200  $\mu\text{L}$  PBS for 2 h; 6-Formylindolo-[3,2-b]-carbazole (FICZ, Tocris) 2  $\mu\text{g}$  in 200  $\mu\text{L}$  PBS for indicated time; indole (Sigma-Aldrich) 100  $\mu\text{g}$  in 200  $\mu\text{L}$  PBS for 12 h; sodium butyrate (Sigma-Aldrich) daily for 5 days with 1 mg per day in 200  $\mu\text{L}$  PBS. For antibiotic treatment, mice were given 1  $\text{g}\cdot\text{l}^{-1}$  metronidazole (Sigma-Aldrich), 0.5  $\text{g}\cdot\text{l}^{-1}$  vancomycin (Sigma-Aldrich), 1  $\text{g}\cdot\text{l}^{-1}$  ampicillin (Sigma-Aldrich), 1  $\text{g}\cdot\text{l}^{-1}$  gentamicin (Sigma-Aldrich) and 1  $\text{g}\cdot\text{l}^{-1}$  neomycin (Sigma-Aldrich) by daily oral gavage of 200  $\mu\text{L}$  in antibiotic solution (100% H<sub>2</sub>O). In parallel with the antibiotic treatment, mice were treated per os with 200  $\text{mg}\cdot\text{l}^{-1}$  amphotericin B of 100  $\mu\text{L}$  in solution (100% H<sub>2</sub>O) to avoid occasional overgrowth of *Candida* spp. For microbiota transfer experiment, the gut microbiota was transferred between groups of mice by initially depleting the native microbiota with a single oral dose of streptomycin (20 mg) 24 h prior the transplantation. Fresh fecal pellets (120 mg) from 5 donor mice were collected and placed in 1 ml of transfer buffer (pre-reduced sterile cold PBS containing 0.05% cysteine HCl (Sigma-Aldrich)). The fecal pellets were homogenized, centrifuged at 800 g for 2 min, and 50  $\mu\text{L}$  fecal supernatant was orally inoculated to recipient mice over the subsequent 15 days for a total of 6 times. All animal experimental protocols were approved by the ethic committee for animal experimentation (APAFIS#3535-2015092416202090).

### Spontaneous Diabetes Incidence

Eight-weeks-old NOD female mice received one injection of mBD14 or scmBD14 (10  $\mu\text{g}$ ) per week during two weeks or similar injections of vehicle (PBS-1% H<sub>2</sub>O). In some conditions, mice were treated (200  $\mu\text{g}$  per injection at day -1, 1, 3, 6 and 9 post mBD14 treatment) with anti-IL4 (11B11) or relevant isotype control. Overt diabetes was defined as two positive urine glucose tests, confirmed by a glycemia >200  $\text{mg}\cdot\text{dl}^{-1}$ . Glukotest kit was purchased from Roche. Glucose tests and measure of glycemia were performed in a blind fashion.

## METHOD DETAILS

### Preparation of Pancreatic Islets

Pancreata were perfused with a solution of collagenase P in HBSS-1% HEPES (0.75  $\text{mg}\cdot\text{ml}^{-1}$ , Roche), then dissected free from surrounding tissues. Pancreata were digested at 37°C for 8 min. Digestion was stopped by adding HBSS-10% FCS-1% EDTA followed by extensive washes. For flow cytometry analysis, islets were isolated on a discontinuous Ficoll PM400 gradient (Sigma-Aldrich) and then cells were released from the islets by incubation at 37°C for 6 min in non-enzymatic cell dissociation solution (Sigma-Aldrich). For islets culture, cytology and RT-qPCR, to avoid potential contamination by exocrine tissue, islets were purified by handpicking in 3 consecutive baths of HBSS-10% FCS supplemented with 1% DNase 1.

### RT-qPCR

Total RNA was isolated using the Nucleospin RNA XS kit (Macherey-Nagel) from a minimum of 100 handpicked islets per mouse. RNA was reverse transcribed to synthesized cDNA using the high capacity cDNA reverse transcription kit (Thermo Fisher) and measurements were performed by qPCR using Takyon ROX SYBR MasterMix dTTP blue (Eurogentec) on a 7900HT Fast System (Applied Biosystems). Resulting levels of fluorescence were submitted to relative quantification by normalization against a housekeeping gene (GAPDH) and expressed as  $2^{-(\Delta\text{CT})}$  values.

### Flow Cytometry

Single cell suspensions were prepared from various tissues and were stained for 30 min at 4°C after Fc $\gamma$ RII/III blocking with anti-CD16/CD32 (Biolegend, 93) monoclonal antibody (mAb). Staining buffer was PBS containing 2% FCS, 0.5% EDTA and 0.1% sodium azide. Surface staining was performed with the following mAbs against: CD45 (eBioscience, 30-F11), CD11b (eBioscience, M1/70), F4/80 (eBioscience, BM8), CD11c (eBioscience, N418), TCR $\beta$  (eBioscience, H57-597), TCR $\gamma/\delta$  (eBioscience, UC7-13D5), CD19 (eBioscience, 1D3), CD206 (Biolegend, C068C2), CD5 (Miltenyi, 53-7.3), CD1d (Biolegend, K253), CD21 (Biolegend, 7E9), CD24 (Biolegend, 30-F1), B220 (Biolegend, RA3-6B2), CD138 (Biolegend, 281-2), TLR2 (Biolegend, CB225), CD127 (Biolegend, A7R34), -CD90.2 (eBioscience, 53-2.1). Lin markers are a mix of anti-CD19, -CD5, -CD3 $\epsilon$ , -B220, -CD11b, and -CD11c mAbs. For measurement of active TGF $\beta$ , cells were surface stained with anti-LAP mAb (eBioscience, TW7-16B4). For cytokine expression, cell suspensions were incubated 5 h at 37°C with the relevant stimulus, if required, in the presence of a protein transport inhibitor cocktail (eBioscience), surface stained, fixed and then intracellularly stained using the intracellular staining kit (Biolegend). For macrophages and DCs, cell suspension was incubated with LPS (1  $\mu\text{g}\cdot\text{ml}^{-1}$ , Sigma-Aldrich) and stained with anti-TNF $\alpha$  (eBioscience, MP6-XT22), -IL-12 (eBioscience, C17.8), -IL-4 (eBioscience, 11B11), -IL-10 (eBioscience, JES5-16E3) and -IL-23 (eBioscience, fc23-cpg). For innate lymphoid cells, cell suspension was incubated with rmlL-23 (10  $\text{ng}\cdot\text{ml}^{-1}$ , Miltenyi) plus PMA/ionomycin (both 500  $\text{ng}\cdot\text{ml}^{-1}$ , Sigma-Aldrich) and stained with anti-IL-22 pAb (Biolegend, poly5164) or control isotype (goat IgG, Biolegend, poly24030). For diabetogenic CD8<sup>+</sup> T cells, cell suspension was incubated with bone-marrow derived DCs loaded with IGRP<sub>206-214</sub> peptide and stained with anti-CD8 $\alpha$  (BD, 53-6.7) and anti-IFN $\gamma$  mAbs (eBioscience, XMG1.2). For B cells, cell suspension was incubated without additional stimulus and stained with anti-IL-4 (eBioscience, 11B11), -IL-10 (eBioscience, JES5-16E3) and -IDO (Biolegend, 2E2/IDO1) mAbs. For regulatory T cell detection, cells were surface stained with anti-TCR $\beta$ , -CD4 (BD, RM4-5), fixed and then stained for Foxp3 (eBioscience, FJK-16s) expression, using the Foxp3 staining kit (eBioscience). For staining of transcription factors RoR $\gamma$ t, GATA3 (eBioscience, B2D and 16E10A23) and ki67 (eBioscience, SolA15), cells were stained using the True-Nuclear Transcription Factor kit (Biolegend). In all experiments dead cells were excluded using Fixable Viability Dye

(eBioscience). Stained cells were analyzed on a Becton Dickinson Fortessa flow cytometer. Data were analyzed with Flowjo v10 software.

### Immunocytology

Handpicked pancreatic islets were seeded on SuperFrost Gold Plus microscope slide. For  $\beta$ -defensin staining, islets were fixed, blocked with goat serum, permeabilized, and stained with anti-insulin pAb (Abcam, ab7842), anti-glucagon mAb (Abcam, ab10988) and anti-mBD14 pAb (Mybiosource, MBS1490249) or anti-hBD3 pAb (Abcam, ab19270), overnight at 4°C. After washing, second-step reagents were applied: anti-guinea pig-AlexaFluor488, anti-mouse-Alexa647 and anti-rabbit-AlexaFluor555 pAbs (Invitrogen). For IL-22 staining, isolated islets were incubated 5 h at 37°C with rIL-23 (10 ng.ml<sup>-1</sup>, Miltenyi) and PMA/ionomycin (both 500 ng.ml<sup>-1</sup>, Sigma-Aldrich) in the presence of a protein transport inhibitor cocktail. Then islets were fixed, blocked with donkey serum, permeabilized and stained with anti-insulin pAb (Abcam), anti-CD5 mAb (Biolegend, 53-7.3) and anti-IL-22 mAb (Biolegend, poly5164), overnight at 4°C. After washing, second-step reagents were applied: anti-guinea pig-AlexaFluor488, anti-rat-Alexa555 and anti-goat-AlexaFluor647 pAbs (Invitrogen). Nuclei were stained with DAPI. Image acquisition was performed on Necker Institute Imaging Facility using a Leica SP8 confocal microscope.

### In Vitro B Cell Culture

B cells were magnetically isolated using MACS cell separation system (anti-biotin beads, Miltenyi). CD19<sup>+</sup> B cells (2x10<sup>5</sup> cells per well) from pancreatic lymph nodes or pancreatic islets of 10-weeks-old female WT or *myd88*<sup>-/-</sup> NOD mice were incubated for 4 days in complete IMDM with growing doses (0.1 to 10  $\mu$ g.ml<sup>-1</sup>) of mBD14 or vehicle. Blocking reagents were added as indicated: neutralizing anti-TLR2 mAb (5  $\mu$ g.ml<sup>-1</sup>, Invivogen), TLR1/2 heterodimer antagonist CU-CTP22 (10  $\mu$ M, Tocris).

### In Vitro Treg Cell Induction

All cells were magnetically isolated using MACS cell separation kit and system (Miltenyi). CD62L<sup>+</sup>CD4<sup>+</sup>CD25<sup>-</sup> BDC2.5 T cells (4x10<sup>4</sup> cells per well) from splenocytes of BDC2.5 TCR transgenic NOD mice were incubated with 2x10<sup>3</sup> myeloid cells (CD11b<sup>+</sup>) and or 2x10<sup>3</sup> B cells (CD19<sup>+</sup>) obtained from pancreatic islets of NOD mice treated with mBD14 (10  $\mu$ g.ml<sup>-1</sup>) or vehicle 4 days earlier. Cell culture was performed for 4 days in complete IMDM with 20 ng.ml<sup>-1</sup> of peptide 1040-51, a mimotope of BDC2.5 T cells.

### In Vitro Pancreatic Islet Culture

Mouse and human (Tebu-bio) pancreatic islets isolated by handpicking were cultured in complete IMDM (10% FBS, 0.6 g.l<sup>-1</sup> L-glutamine, 100 U.ml<sup>-1</sup> penicillin streptomycin, 100  $\mu$ M 2-mercaptoethanol, 4.5 g.l<sup>-1</sup> D-Glucose). In some experiments, islets were treated with: rmlL-22 (100 ng.ml<sup>-1</sup>, Biolegend) for 4 h; FICZ (50 ng.ml<sup>-1</sup>, Tocris) for 12 h; rmlL-23 (20 ng.ml<sup>-1</sup>, Miltenyi) for 18 h; sodium butyrate (1 mg.ml<sup>-1</sup>, Sigma-Aldrich) for 48 h with or without neutralizing anti-IL-22 mAb (1  $\mu$ g.ml<sup>-1</sup>, IL22JOP, eBioscience).

### Cytokine Quantification

The level of IL-23 and IL-22 in the serum was determined using commercial ELISA kit (Biolegend).

### RNAseq Gene Expression Profiling

Total RNA were isolated from pancreatic islets (>150) using the RNeasy Kit (QIAGEN) including a DNase treatment step. RNA quality was assessed using RNA Screen Tape 6000 Pico LabChips with the Tape Station (Agilent Technologies) and RNA concentration was measured by spectrophotometry using the Xpose (Trinean). RNAseq libraries were prepared starting from 1  $\mu$ g of total RNA using the TruSeq Stranded mRNA LT Sample Prep Kit (Illumina) as recommended by the manufacturer. Half of the oriented cDNA produced from the poly-A<sup>+</sup> fraction was PCR amplified (11 cycles). The RNAseq libraries were sequenced on an Illumina HiSeq2500 (Paired-End sequencing 130x130 bases, High Throughput Mode). A mean of 23 million of paired-end reads was produced per library sample (between 21 to 25 million of passing filter reads). The generated data were analyzed using the Ingenuity Pathway Analysis software (Qiagen).

### AHR Ligand Activity Measurement

The BioDetection Systems Company performed experiments to determine AHR ligand activity in the serum using a reporter assay system (PAH-CALUX bioassay) (Pieterse et al., 2013). AHR activity in stool samples was determined in the laboratory using the H1L1.c2 cell line, containing a stably integrated dioxin-response element (DRE)-driven firefly luciferase reporter plasmid pGudLuc1.1, as described previously (Lamas et al., 2016; Zhao et al., 2013).

### Analysis of AHR Ligand Composition

The concentrations of Indole-3-Lactic acid, Indole-3-aldehyde, Indole-3-Acetic acid in the serum and the caecal content of mice were determined by a specific method using HPLC-coupled to high resolution mass spectrometry. This quantitative method has been validated analytically on both types of samples in order to meet the criteria FDA Guidance for Industry.

### 16S rDNA Gene Sequencing

Murine stools were frozen at  $-80^{\circ}\text{C}$  immediately after emission and stored until further processing. Then, as previously described (Lamas et al., 2016), feces samples were weighed and then resuspended for 10 min at room temperature in 250  $\mu\text{l}$  of 4 M guanidine thiocyanate in 0.1 M Tris (pH 7.5) (Sigma-Aldrich) and 40  $\mu\text{l}$  of 10% N-lauroyl sarcosine (Sigma-Aldrich). After the addition of 500  $\mu\text{l}$  of 5% N-lauroyl sarcosine in 0.1 M phosphate buffer (pH 8.0), the 2-ml tubes were incubated at  $70^{\circ}\text{C}$  for 1 h. One volume (750 ml) of a mixture of 0.1- and 0.6-mm-diameter silica beads (Sigma-Aldrich) (previously sterilized by autoclaving) was added, and the tube was shaken at 6.5 m/s three times for 30 s each in a FastPrep (MP Biomedicals) apparatus. Polyvinylpyrrolidone (15 mg) was added to the tube, which was then vortexed and centrifuged for 5 min at 20,000g. After recovery of the supernatant, the pellets were washed with 500  $\mu\text{l}$  of TENP (50 mM Tris (pH 8), 20 mM EDTA (pH 8), 100 mM NaCl, 1% polyvinylpyrrolidone) and centrifuged for 5 min at 20,000g, and the new supernatant was added to the first supernatant. The washing step was repeated two times. The pooled supernatant (about 2 ml) was briefly centrifuged to remove particles and then split into two 2-ml tubes. DNA was isolated from the feces of the various mouse strains using the Nucleospin DNA stool (Macherey-Nagel). Microbial diversity was determined for each sample by targeting a portion of the ribosomal genes. A 16S rDNA gene fragment comprising the V3 and V4 hypervariable regions (16S (sense) 5'-TACGGRAGGCAGCAG-3' and (antisense) 5'-CTACCNGGGTATCTAAT-3') was amplified using an optimized and standardized 16S-amplicon-library preparation protocol (Metabio, GenoScreen). Briefly, 16S rDNA gene PCR was performed using 5 ng genomic DNA according to the manufacturer's protocol (Metabio) using 192 bar-coded primers (Metabio MiSeq Primers) at final concentrations of 0.2  $\mu\text{M}$  and an annealing temperature of  $50^{\circ}\text{C}$  for 30 cycles. The PCR products were purified using an Agencourt AMPure XP-PCR Purification system (Beckman Coulter), quantified according to the manufacturer's protocol, and multiplexed at equal concentrations. Sequencing was performed using a 300-bp paired-end sequencing protocol on an Illumina MiSeq platform (Illumina) at GenoScreen. Raw paired-end reads were subjected to the following process: (1) quality-filtering using the PRINSEQ-lite PERL script38 by truncating the bases from the 3' end that did not exhibit a quality  $<30$  based on the Phred algorithm; (2) paired-end read assembly using FLASH39 (fast length adjustment of short reads to improve genome assemblies) with a minimum overlap of 30 bases and a 97% overlap identity; and (3) searching and removing both forward and reverse primer sequences using CutAdapt, with no mismatches allowed in the primers sequences. Assembled sequences for which perfect forward and reverse primers were not found were eliminated.

### QUANTIFICATION AND STATISTICAL ANALYSIS

#### 16S rDNA Gene Sequence Analysis

The sequences were demultiplexed, quality-filtered using the 'quantitative insights into microbial ecology' (QIIME, version 1.8.0) software package (Caporaso et al., 2010), and the forward and reverse Illumina reads were joined using the fastq-join method (<http://code.google.com/p/ea-utils>). The sequences were assigned to OTUs using the UCLUST algorithm (Edgar, 2010) with a 97% threshold of pairwise identity and classified taxonomically using the Greengenes reference database (McDonald et al., 2012). Rarefaction was performed (30,000 sequences per sample) and used to compare the abundances of OTUs across samples.

#### Statistical Analysis

Diabetes incidence was plotted according to the Kaplan-Meier method. Incidences between each group were compared with the log-rank test. Reported values are median  $\pm$  interquartile range as indicated. Comparison between each group was performed using the non-parametric Mann-Whitney U-test. P values  $< 0.05$  were considered statistically significant. All data were analyzed using GraphPad Prism v6 software.

### DATA AND SOFTWARE AVAILABILITY

The RNA-seq data reported in this paper is published in Mendeley Data (<https://doi.org/10.17632/4g2jdjxcff.1>).